The osteology and phylogenetic position of the loricatan (Archosauria: Pseudosuchia) *Heptasuchus clarki,* from the ?Mid-Upper Triassic, southeastern Big Horn Mountains, Central Wyoming (U.S.A.)

Sterling J Nesbitt [Corresp., 1], **John M Zawiskie** [2, 3], **Robert M Dawley** [4]

[1] Department of Geosciences, Virginia Tech, Blacksburg, Virginia, United States

[2] Cranbrook Institute of Science, Bloomfield Hills, Michigan, United States

[3] Department of Geology, Wayne State University, Detroit, Michigan, United States

[4] Department of Biology, Ursinus College, Collegeville, Pennsylvania, United States

Corresponding Author: Sterling J Nesbitt
Email address: sjn2104@vt.edu

Loricatan pseudosuchians (known as “rauisuchians”) typically consist of poorly understood fragmentary remains known worldwide from the Middle Triassic to the end of the Triassic Period. Renewed interest and the discovery of more complete specimens recently revolutionized our understanding of the relationships of archosaurs, the origin of Crocodylomorpha, and the paleobiology of these animals. However, there are still few loricatans known from the Middle to early portion of the Late Triassic and the forms that occur during this time are largely known from southern Pangea or Europe. *Heptasuchus clarki* was the first formally recognized North American “rauisuchian” and was collected from a poorly sampled and disparately fossiliferous sequence of Triassic strata in North America. Exposed along the trend of the Casper Arch flanking the southeastern Big Horn Mountains, the *Heptasuchus clarki* type locality occurs within a sequence of red beds above the Alcova Limestone and Crow Mountain formations within the Upper Chugwater Group. The age of the type locality is poorly constrained to the Middle – early Late Triassic and is likely similar to or just older than that of the Popo Agie Formation assemblage from the western portion of Wyoming. The holotype consists of associated cranial elements found in situ, and the referred specimens consist of crania and postcrania. Thus, about 50% of the osteology of the taxon is preserved. All of the pseudosuchian elements collected at the locality appear to belong to *Heptasuchus clarki* and the taxon is not a chimera as previously hypothesized. *Heptasuchus clarki* is distinct from all other archosaurs by the presence of large, posteriorly directed flanges on the parabasisphenoid and a distinct, orbit-overhanging postfrontal. Our phylogenetic hypothesis posits a sister-taxon relationship between *Heptasuchus clarki* and the Ladinian-aged *Batrachotomus*

kupferzellensis from current-day Germany within Loricata. These two taxa share a number of apomorphies from across the skull and their position further supports ‘rauisuchian’ paraphyly. A minimum of four individuals of *Heptasuchus* are present at the type locality suggesting that a group of individuals died together, similar to other aggregations of loricatans (e.g., *Heptasuchus*, *Batrachotomus*, *Decuriasuchus*, *Postosuchus*).

The osteology and phylogenetic position of the loricatan (Archosauria: Pseudosuchia) *Heptasuchus clarki,* from the? Mid-Upper Triassic, southeastern Big Horn Mountains, Central Wyoming (U.S.A.)

Sterling J. Nesbitt[1], John M. Zawiskie[2] and Robert M. Dawley[3]

[1]Department of Geosciences, Virginia Tech, Blacksburg, VA 24061, U.S.A.
[2]Cranbrook Institute of Science, 39221 Woodward Ave, Bloomfield Hills, MI 48303 and Department of Geology Wayne State University, Detroit, MI 48202, U.S.A.
[3]Department of Biology, Ursinus College PO Box 1000 Collegeville, PA 19426, U.S.A.

Corresponding Author:
Sterling J. Nesbitt[1]
926 W. Campus Dr. Derring Hall, Virginia Tech, Blacksburg, VA, U.S.A.
Email address: sjn2104@vt.edu

Abstract

Loricatan pseudosuchians (known as “rauisuchians”) typically consist of poorly understood fragmentary remains known worldwide from the Middle Triassic to the end of the Triassic Period. Renewed interest and the discovery of more complete specimens recently revolutionized our understanding of the relationships of archosaurs, the origin of Crocodylomorpha, and the paleobiology of these animals. However, there are still few loricatans known from the Middle to early portion of the Late Triassic and the forms that occur during this time are largely known from southern Pangea or Europe. *Heptasuchus clarki* was the first formally recognized North American “rauisuchian” and was collected from a poorly sampled and disparately fossiliferous sequence of Triassic strata in North America. Exposed along the trend of the Casper Arch flanking the southeastern Big Horn Mountains, the *Heptasuchus clarki* type

locality occurs within a sequence of red beds above the Alcova Limestone and Crow Mountain formations within the Upper Chugwater Group. The age of the type locality is poorly constrained to the Middle – early Late Triassic and is likely similar to or just older than that of the Popo Agie Formation assemblage from the western portion of Wyoming. The holotype consists of associated cranial elements found in situ, and the referred specimens consist of crania and postcrania. Thus, about 50% of the osteology of the taxon is preserved. All of the pseudosuchian elements collected at the locality appear to belong to *Heptasuchus clarki* and the taxon is not a chimera as previously hypothesized. *Heptasuchus clarki* is distinct from all other archosaurs by the presence of large, posteriorly directed flanges on the parabasisphenoid and a distinct, orbit-overhanging postfrontal. Our phylogenetic hypothesis posits a sister-taxon relationship between *Heptasuchus clarki* and the Ladinian-aged *Batrachotomus kupferzellensis* from current-day Germany within Loricata. These two taxa share a number of apomorphies from across the skull and their position further supports 'rauisuchian' paraphyly. A minimum of four individuals of *Heptasuchus* are present at the type locality suggesting that a group of individuals died together, similar to other aggregations of loricatans (e.g., *Heptasuchus*, *Batrachotomus*, *Decuriasuchus*, *Postosuchus*).

Introduction

During the Middle and Late Triassic, large pseudosuchians archosaur predators appeared across Pangea and came in a variety of forms. These forms included long-snouted phytosaurs (Stocker and Butler 2013), sailed-back poposauroids (Nesbitt 2003; 2005; 2011; Butler et al. 2011; Nesbitt et al. 2011), short-faced ornithosuchids (von Baczko and Ezcurra 2013), and quadrupedal, large headed 'rauisuchians' – a group that has been traditionally classified together. 'Rauisuchians' have been found in nearly every well-sampled Middle to Upper Triassic deposit, but the anatomy and the relationships of these pseudosuchians remains

55 debated (Gower 2000; Brusatte et al. 2008; 2010; Nesbitt 2011; Nesbitt et al. 2013a). Namely, it
56 is not clear if these 'rauisuchians' represent a natural group (traditional hypothesis; Brusatte et
57 al. 2008; 2010), a grade leading to crocodylomorphs (Nesbitt 2011), or a combination of
58 subclades and grades spread across Pseudosuchia (Nesbitt 2011). Luckily, over the past 20
59 years, huge headway has been made in uncovering their anatomy and relationships through the
60 discovery of new taxa (e.g., *Batrachotomus kupferzellensis*; Gower 1999; Gower and Schoch
61 2009; *Postosuchus alisonae*, Peyer et al. 2008; *Decuriasuchus quartacolonia*, França et al.
62 2011; 2013; *Viveron haydeni*, Lessner et al. 2016); *Mandasuchus tanyauchen*, Butler et al.
63 2018), or new specimens of previously named taxa (e.g., *Arizonasaurus babbitti*, Nesbitt 2003;
64 2005; *Prestosuchus chiniquensis*, Roberto-Da-Silva et al. 2018; Mastrantonio et al. 2019;
65 *Poposaurus gracilis,* Schachner et al. 2019) and revised and detailed descriptions (e.g.,
66 *Rauisuchus tiradentes*, Lautenschlager and Rauhut 2015; *Postosuchus kirkpatricki*, Weinbaum
67 2011; 2013; *Luperosuchus fractus*, Nesbitt and Desojo 2017; *Prestosuchus chiniquensis*,
68 Desojo et al. 2020; *Ticinosuchus ferox*, Lautenschlager and Desojo 2011).
69 'Rauisuchians' from the western central Pangea (now the western portion of North
70 America) have been instrumental in helping unravel the relationship of the group and
71 pseudosuchians. Remains of 'rauisuchians' occur through the Chinle Formation and Dockum
72 Group (Long and Murry 1995) and now it is clear that nearly all of those taxa or unnamed forms
73 can be sorted into two major groups, the Poposauroidea (*Poposaurus gracilis* and abundant
74 shuvosaurids) and the rauisuchids (*Postosuchus kirkpatricki* and like forms such as *Viveron*
75 *haydeni*). To date, these two groups represent highly derived forms within Pseudosuchia and
76 western North America is clearly lacking early diverging paracrocodylomorphs (e.g.,
77 *Mandasuchus tanyauchen* from Tanzania), early diverging loricatans (South American or Africa
78 forms like *Prestosuchus chiniquensis*), or more 'middle' loricatan forms like *Batrachotomus*
79 *kupferzellensis* (from Germany). Out of all of the forms from current-day western North America,
80 only one possible taxon fits into this gap. This important taxon, *Heptasuchus clarki*, was the first

formally recognized ‘rauisuchian’ in North America but was only named and briefly described (Dawley et al. 1979). Moreover, *Heptasuchus clarki* occurs in Triassic sediments of central Wyoming, a place that few vertebrates of this age have been found. Since its naming, Long and Murry (1995) reevaluated parts of its anatomy and considered the taxon as a possible synonym of *Poposaurus* whereas it has been mentioned as a ‘rauisuchian’, but not formally described or placed into a phylogenetic context.

In this paper, we fully detail the osteology of *Heptasuchus clarki* by describing the holotype skull and associated postcranial material from the type locality bone bed, provide details on a revised geologic setting and age for the taxon and evaluate its evolutionary affinities with other pseudosuchians.

Geological Setting: locality, regional, age, and associated assemblage

The *Heptasuchus clarki* type locality (= Clark Locality of Dawley et al. 1979) occurs within a sequence of red beds near the Red Wall Valley on the southeastern flank the Big Horn Mountains in central Wyoming (Natrona County) within the Chugwater Group (Fig. 1). The *Heptasuchus clarki* bonebed occurs in a sequence of highly calcareous intraformational conglomerates, thin ripple marked highly bioturbated sandstone beds, silty micrites and reddish brown to dusky red and intercalated green mudstones. All in situ material of *Heptasuchus clarki* (e.g., partial skull, some postcrania) (see below) was derived from 2 to 30 cm thick red mudstone / weathered red regolith (Fig. 1) which is exposed across the bonebed. All cranial elements were found in situ disarticulated but closely aligned in a one-half square meter area in this red mudstone (Fig. 1). Nearly all of the surface collected specimens of *Heptasuchus clarki* and the associated assemblage were collected from the weathered red regolith. With the exception of a lungfish tooth (UW 11567) and a small centrum, no other bones were found below the red mudstone in the underling green mudstone, thin limestone, or conglomerate.

106 The depositional setting at the locality is inferred to have been a vegetated distal
107 floodplain environment, periodically experiencing sheet floods and the development of
108 ephemeral ponds and lakes. The sheet floods generated the intraformational conglomerates
109 with calcareous nodules and mudstone clasts scoured from soils on the flood plain sediments.
110 The limestone microconglomerates at the *Heptasuchus clarki* site indicate high-energy flood
111 events and the silty micrites suggest post-flood deposition in lakes and ponded, abandoned
112 channels.
113 The inclusion of the *Heptasuchus clarki* bonebed into a formal stratigraphic unit in the
114 Chugwater Group on the southeastern flank the Big Horn Mountains has been challenging and
115 debated. These debates are the result of a number of factors including the lack of continuous
116 outcrops in the area, the unique sedimentology of the unit that the *Heptasuchus clarki* bonebed
117 lies in, the lack of clear lithostratigraphic signatures of other Triassic formations across
118 Wyoming and the lack of clear, and useful fossils for biostratigraphic correlation. It is clear that
119 *Heptasuchus clarki* type locality lies well above the Red Peak Formation and the Alcova
120 Limestone given that both crop out locally within a kilometer and can be easily mapped. It is
121 also clear that *Heptasuchus clarki* bonebed lies about 50 meters from the top of the Alcova
122 Limestone and ~10 meters below the Gypsum Springs Formation (Fig. 1) which lies on a nearby
123 butte (~30 meters away).
124 The strata between the Alcova Limestone and the Gypsum Springs Formation have
125 been assigned to a number of stratigraphic units. The Crow Mountain Sandstone lies directly on
126 the Alcova Limestone and consists of sandstones with current crossbedding (Cavaroc and
127 Flores 1991). The fluvial and lacustrine sediments stratigraphically above the Crow Mountain
128 Sandstone, but below the Gypsum Springs Formation have been assigned to the Popo Agie
129 Formation based on the sequence and general lithology (Picard, 1978) or by fossil vertebrates
130 from this area (Dawley et al. 1979; Lucas et al. 2002) whereas geologists working in the same
131 area assigned these strata to the ‘unnamed red beds’ and hypothesize that the Popo Agie

Formation in this region was removed by Jurassic erosion and is not present in the area (Cavaroc and Flores 1991; Irmen and Vondra, 2000). The sedimentology and sequence of these strata in question are demonstrably different from that of the Popo Agie Formation further west. High and Picard (1965) and Cavaroc and Flores (1991) interpreted the lenticular and sheet sandstones in the lower portion of the unnamed red beds as channel and splay deposits of a westward prograding fluvial deltaic plain, comparable to equivalent facies of the Jelm Formation (Picard, 1978), specifically the Sips Creek Member of the Jelm Formation of south-central Wyoming (Pipiringos and O'Sullivan 1978; Cavaroc and Flores 1991). Cavaroc and Flores (1991) considered the calcareous sandstones, silty micrites and red mudstones of the upper portion of the unnamed red beds to be lake deposits that formed in passive areas of a well-integrated alluvial plain. This juxtaposition of fluvial deltaic in the lower portion and the fossiliferous fluvial - lacustrine facies also characterizes the relationship between the Jelm Formation and vertebrate-bearing lower portion of the Popo Agie Formation in the Wind River Range (High and Picard, 1969, Picard, 1978). The *Heptasuchus clarki* bonebed lies in the fluvial - lacustrine facies in the upper 10 meters of the unnamed red beds and there appears to be a clear transition located just stratigraphically below the locality. Whether this upper part of the unnamed red beds is equivalent to the Popo Agie Formation or part of the formation is not clear.

Age:

The age of the *Heptasuchus clarki* bonebed within the unnamed red beds is poorly constrained because of the lack of unambiguous correlations and lack of biostratigraphically informative fossils. No direct dating methods have been used in the area, but there is a lower bound and upper bound. The Alcova Limestone from the local area was dated as Spathian or earliest Anisian (Aegean) age as suggested by the position of the 87Sr/86Sr data on the global marine 87Sr/86Sr curve (Lovelace and Doebbert 2015). The sequence is capped by the Gypsum Springs Formation and this has been assigned a Jurassic age (High and Picard 1965;

158 Pipiringos and O'Sullivan 1978). Thus, the Crow Mountain Sandstone and the unnamed red
159 beds are constrained to Middle-Upper Triassic and this has been suggested by many (High and
160 Picard, 1969; Picard, 1978; Pipiringos and O'Sullivan 1978; Cavaroc and Flores 1991).
161 Further constraints on the age of the unnamed red beds was based on lithostratigraphic
162 correlation to units with biostratigraphically informative vertebrates. Historically, this region was
163 correlated with the Upper Triassic Popo Agie Formation from the Wind River Range and this
164 formation has a rich vertebrate record comprised of phytosaurs (Lees, 1907, Mehl 1915, Lucas,
165 Heckert & Rinehart), metoposaurids (Branson & Mehl, 1929), dicynodonts (Williston, 1904), and
166 a paracrocodylomorph (Mehl, 1915). The presence of metoposaurids and *Parasuchus* has been
167 taken to indicate an early Late Carnian age (Paleorhinus Biochron of Lucas 1998; Lucas et al,
168 2007); however, the general validity of such biochrons is currently a contentious issue (Rayfield,
169 Barrett & Milner, 2009). Regardless, no clear Popo Agie Formation taxa have been found at the
170 *Heptasuchus clarki* bonebed; no phytosaur teeth and osteoderms and large temnospondyl
171 dermal fragments that are common throughout the Popo Agie Formation were found directly at
172 the locality. Metoposaurid dermal bone fragments and phytosaur teeth (UW 11571), have been
173 found in the area (~5 km) of the *Heptasuchus clarki* bonebed but it is not clear if these occur in
174 the same stratigraphic unit. Furthermore, a *Hyperodapedon* rhynchosaur was found to the north
175 of the *Heptasuchus clarki* bonebed (Lucas et al. 2002) and the presence of this genus of
176 rhynchosaur was used to argue for an Upper Triassic age for the strata in this area (including
177 the *Heptasuchus clarki* bonebed). However, the correlation of the *Hyperodapedon* locality and
178 the *Heptasuchus clarki* bonebed is not clear and no diagnostic rhynchosaur remains have been
179 found at the *Heptasuchus clarki* bonebed.
180 Using what little age constraints are available, the age of the *Heptasuchus clarki*
181 bonebed could range from Middle to Upper Triassic. Our best hypothesis concerning the age is
182 that the upper portion of the unnamed red beds at the *Heptasuchus clarki* type locality is

equivalent to or just older than that of the early Late Triassic Popo Agie Formation assemblage from western Wyoming.

Associated assemblage:

The *Heptasuchus clarki* bonebed has produced the remains of at least four individuals of *Heptasuchus clarki* (see below) as well as bones of much smaller vertebrates; these specimens are represented in collections at UW (e.g., UW 11568-115670), TMM, USMN, and NMMNH. Of the larger vertebrates, we hypothesize that all of the material pertains to *Heptasuchus clarki* although none of the postcrania is part of the holotype. The criticism that the material represents a mix of a 'rauisuchian' and generically indeterminate phytosaur (Wroblewski 1997) is not supported here given that 1) we have not seen clear evidence that there is more than one 'rauisuchian' based on comparisons with *Batrachotomus kupferzellensis* and 2) we have not positively identified any phytosaur crania, teeth, or postcrania material. Of the smaller vertebrates, vertebrae, limb bones, small teeth, and other fragments were abundant on the surface, but nearly all of these elements are broken (i.e., vertebral centra halves, limb bone end). A single lungfish tooth was found at the locality (UW 11567). The identification of this material is ongoing and will be the subject of another publication.

Systematic Paleontology

ARCHOSAURIA Cope, 1869 sensu Gauthier 1986

SUCHIA Krebs 1976 sensu Sereno et al. 2005

Heptasuchus clarki Dawley, Zawiskie, and Cosgriff 1979

"*Heptasuchus*"; Benton 1986: 298

"*Heptasuchus clarki*"; Bonaparte 1984: 213

"*Heptasuchus clarki*"; Parrish 1993: 301

"*Heptasuchus clarki*"; Juul 1994: 10

209 "*Heptasuchus clarkei*"; Long and Murry 1995: 154

210 "*Heptasuchus clarki*"; Lucas 1998: 364

211 "*Heptasuchus clarki*"; Alcober 2000: 313

212 "*Heptasuchus clarki*"; Gower 2000: 451

213 "*Heptasuchus clarki*"; Lucas et al. 2002: 150

214 "*Heptasuchus*"; Sulej 2005: 85

215 "*Heptasuchus*"; Lucas et al. 2007: 222

216 "*Heptasuchus*"; Peyer et al 2008: 363

217 "*Heptasuchus*"; Brusatte et al. 2010: 10

218 "*Heptasuchus clarki*"; de França et al. 2013: 473

219 "*Heptasuchus clarki*" Nesbitt et al. 2013a: 246

220

221 **Holotype:** UW 11562-A-S, partial skull: right premaxilla (A); right maxilla (B); left maxilla (C);
222 right jugal (D); left jugal (E); right nasal (F); right postfrontal, postorbital, partial frontal, and
223 prefrontal (G); occiput and braincase (H); left palatine (K); pterygoid? (L); pterygoid fragment
224 (M); fragment of hyoid? (N); unidentified skull fragments (O-R); loose teeth (UW ll562-AA
225 through -AI). Here, the holotype is restricted to the cranial elements found in situ in quad A-3
226 (Fig. 2). No skull element is duplicated and the relative similar sizes of the elements suggest
227 that the remains are from a single individual.

228

229 **Referred material:** quadrate head (UW 11563-AD); ventral condyles of left quadrate (UW
230 11563-AF, UW 11563-H); anterior cervical vertebra (UW ll562-T) ; posterior cervical centrum
231 (UW ll564-A); posterior trunk vertebra (TMM unnumbered); neural spine of a cervical-trunk
232 vertebra (UW ll562-CX); presacral neural spine (UW ll562-V); presacral neural spine (UW ll562-
233 CT); anterior caudal vertebra (UW ll562-U); distal caudal vertebra (UW 11562-BW; UW ll563-A-
234 C); osteoderm (TMM unnumbered); right partial scapula (UW 11565-E); right partial scapula

(UW 11566-B); partial left coracoid (UW 11566); proximal portion of left humerus (UW 11565-A); left humerus (UW ll563-U); proximal portion of the radius (UW 11562-DM); distal portion of the radius (UW 11562-DI; UW 11562-DF); right ulna (UW 11562-W); left ulna in (UW 11562-X); distal ends of ulnae (UW ll563-V; UW ll565-C); left pubis (UW 11562-Y); ilium fragment (UW 11563-Y); pubic peduncle of the right ilium (UW 11563-Z); left pubis (UW 11562-Y); proximal portion of the right ischium (UW 11564-B); proximal portion of a right femur (UW 11563-B); distal portion of the right femur (UW 11563-A); left tibia (UW 11562-Z); proximal portion of a right fibula (UW 11566-S); distal portion of the right fibula (UW 11566-R); proximal end of metatarsals (UW 11562-DH, UW 11562-DHU, UW 11562-DR); ungual (UW 11562-DT).

Type Locality: Clark locality; section 2l, TAON, RSQW, E Natrona County, Red Wall Valley, southern Big Horn Mountains, Wyoming, U.S.A.

Stratigraphic Occurrence: unnamed red beds of the Chugwater Group. Age = ?Middle Triassic to Upper Triassic (see above for details).

Differential diagnosis: *Heptasuchus clarki* differs from all other suchians except for *Batrachotomus kupferzellensis* in processing the following combination of character states: exit for cranial nerve V within prootic; a depression on the anterolateral surface on the ventral end of the postorbital (character 416- state 1); a deep depression on the posterodorsal portion of the lateral surface of the ventral process of the postorbital (418-2); a distinct fossa with a rim present on the nasal at the posterodorsal corner of the naris (422-1); the anteroventral corner of the maxilla extensively laterally overlaps the posteroventral corner of the premaxilla (423-1); and an anteroposteriorly trending ridge on the lateral side of the jugal asymmetrical dorsoventrally where the dorsal portion is more laterally expanded (425-1). Furthermore, *Heptasuchus clarki* and *Batrachotomus kupferzellensis* share the following two homoplastic characters within

Archosauria: Concave anterodorsal margin at the base of the dorsal process of the maxilla (25-1); and dorsolateral margin of the anterior portion of the nasal with distinct anteroposterior ridge on the lateral edge (35-1: Rauisuchidae synapomorphy also).

Heptasuchus clarki differs from *Batrachotomus kupferzellensis* in that *Heptasuchus clarki* lacks a division in the fossa between the basitubera and basipterygoid processes (=median pharyngeal recess) of the parabasisphenoid, the presence of a huge processes on the posterior portion of the basipterygoid processes*; paroccipitals processes more broadly expanded distally; no kink in the ventral process of the postorbital (note, not all *Batrachotomus kupferzellensis* specimens have the kink e.g., SMNS 52970); anterior portion of the maxilla is less expand and has a smaller foramen between maxilla and the premaxilla; palatal process of premaxilla is more expanded medially; palatal process of the maxilla continuous with anterior edge of maxilla (the palatal process is hidden under a flange of bone laterally in *Batrachotomus kupferzellensis*); and the anterolateral corner of postfrontal of *Heptasuchus clarki* is blunt and squared off in dorsal view*. Asterisks denote autapomorphies of *Heptasuchus clarki*.

Ontogenetic status: The ontogenetic age of the specimens of *Heptasuchus clarki* are difficult to assess given the holotype contains only skull elements and the postcrania of the taxon has poor association with cranial or other postcranial remains. An ontogenetic age assessment based on the skull (i.e., fusion events) is not reliable in archosaurs (Bailleul et al. 2016). With the exception of a complete tibia and nearly complete ulna, no other limb bones, like the femoral fragments have a midshaft that could be used for histological analysis. Fragments of limb bones are available, even so, identification of the element based on a limb shaft is difficult and the orientation of the fragments and overall size of the limb would be difficult to assess for comparative purposes. Of the few vertebrae recovered, all neurocentral sutures appear to be fully closed (Brochu 1996; Irmis 2007). This is clear in the partial cervicals, trunk and anterior caudal vertebrae. Based on this cursory assessment, the specimens of *Heptasuchus clarki* are

not young individuals, but their ontogenetic stage is largely unconstrained with the available evidence.

Notes: The original holotype of *Heptasuchus clarki* (Dawley et al.1979) was amended by Zawiskie and Dawley (2003), who restricted it to the in situ cranial material collected in 1977 in quads A-1 and A-2 of the excavation grid at the Clark locality (see grid in Dawley, 1979 or supplementary materials) following the criticism that the taxon may represent a chimera (Wroblewski 1997). Much of the bonebed was weathered and many bone fragments littered the ground and these specimens were collected in 1977-1979 and in 2009-2010. The association of the postcranial elements is not known but are assigned to *Heptasuchus clarki* based on similarity among elements and similarity to the almost completely known anatomy of *Batrachotomus kuperferzellensis* (Gower 1999; Gower and Schoch 2009); we are assuming that all of the archosaur material that is similar in comparative size emanates from a single taxon of loricatan. Therefore, we only refer material to the taxon and do not create paratype specimens. The locality has a minimum number of four individuals of similar size, as deduced from the number of right distal ends of the ulna.

Comparative Morphological Description

General skull: Most of the skull of the holotype specimen (UW ll562-A through -S) was recovered as separate, disarticulated bones, except for the postorbital-postfrontal-frontal prefrontal section. The total complement of bones is by no means complete and several elements (lacrimal, squamosal, quadratojugal, and quadrate) are not represented on either the right or left side. However, sufficient material is preserved to provide a reconstruction of most areas of the skull and skeleton (Fig. 3). Only the quadrate region is totally unknown, and the palate is represented only by a single fragment. We estimate the skull to be about 56 cm long.

312 The following describes the general aspect of the skull and details of each element are
313 included below. The skull is long and narrow with the preorbital (tooth-bearing) length about
314 two-thirds that of the total length. In lateral view (Fig. 3), the lower margin of the skull forms,
315 roughly, an obtuse angle whose apex points ventrally and is located at the level of the sixth
316 maxillary tooth. There are three premaxillary and nine maxillary teeth preserved. A possible
317 small accessory antorbital fenestra exists between the premaxilla and the maxilla (see more
318 details below), but this area is damaged. Posteriorly, a moderately large antorbital fenestra lies
319 in a recessed antorbital fossa. The orbit is 'keyhole shaped,' and this configuration reflects the
320 expansion of the lower part of the enlarged infraorbital fenestra. In the area of the nasal, the
321 lateral borders of the skull roof form a pair of elevated ridges, which flank a shallow depression
322 in the center of the dorsal surface of the skull roof. The supratemporal fenestra is small,
323 triangular, and surrounded by a supratemporal fossa.
324
325 **Premaxilla:** The premaxilla is only known from the right side (UW ll562-A; Fig. 4E-F) and lacks
326 the anterior portion of the first preserved alveolus, the posterior end of the third alveolus, and
327 the complete anterodorsal (=narial) process. *Heptasuchus clarki* was originally described as
328 having three premaxillary teeth but, the tooth-bearing margin is incomplete. At least three
329 premaxillary teeth are present but the exact number of premaxillary teeth is unknown. The body
330 of the premaxilla is rounded laterally and does not preserve a distinct narial fossa anteroventral
331 to the external naris, a distinct feature of the premaxilla of *Batrachotomus kupferzellensis*. No
332 foramina are apparent on the premaxilla, but this is possibly the result of a highly fractured
333 surface.
334 Two prominent processes are preserved, a palatal and a posterodorsal (=maxillary)
335 processes. The posterodorsal process is straight, slender, and projects 30^{o} posterodorsally. The
336 posteroventral edge of the process forms a concave margin that frames part of the posterior
337 margin of the external naris. The relative length of the process compared to the length of the

premaxillary body is similar to that of *Postosuchus kirkpatricki* (TTUP 9000) and *Rauisuchus tiradentes* (BSPG AS XXV-60-121), longer than that of *Batrachotomus kupferzellensis* (Gower 1999), and is much shorter than the longer, more robust, and arched subnarial processes present in *Saurosuchus galilei* (PVSJ 32) and *Luperosuchus fractus* (PULR 04; Nesbitt and Desojo 2017). A small foramen is located in the body of the premaxilla ventral to the base of the posterodorsal process. The base of the posterodorsal process is not laterally expanded into a bulge posteroventral of the external naris as in *Rauisuchus tiradentes* (BSPG AS XXV-60-121; Lautenschlager and Rauhut 2015), *Vivaron haydeni* (Lessner et al. 2016), *Postosuchus kirkpatricki* (Weinbaum 2011), and *Polonosuchus silesiacus* (Sulej 2005).

The palatal process is a broad, flat, transversely oriented sheet of bone that originates at the dorsal of the tooth row and projects medially to contact its antimere. Ventrally, the palatal process forms the base of a ventrally opening fossa. The process forms the anterior edge of the anterior portion of the palate, as in *Saurosuchus galilei* (Alcober 2000). The posterior edge of the process articulates with the vomer.

Maxilla: The posterior two-thirds of the right maxilla (UW ll562-B; Fig. 4C-D) and the anterior half of the tooth-bearing portion of the left maxilla (UW ll562-C; Fig. 4A-B) are present in the holotype of *Heptasuchus clarki*. Only the base of the dorsal (=ascending) process is preserved. The left maxilla preserves the first six alveoli and the preserved portion of the right maxilla preserves eight alveoli. As reconstructed (Fig. 3; Dawley et al. 1979), a complete maxilla would have a minimum of ten teeth, as determined by overlap of the two preserved maxillae; the alveolus tooth from the left maxilla fragment is considered to be equivalent to the anteriormost alveolus of the right maxillary fragment. As reconstructed, the maxilla is a massive, rectangular bone with a deep body similar to that of *Fasolasuchus tenax* (PVL 3851), *Batrachotomus kuperferzellensis* (SMNS 80260) and *Saurosuchus galilei* (PVSJ 32).

363 The anterior portion of the maxilla is well preserved. The lateral surface is rather flat and
364 not laterally expanded. The anterior margin of the maxilla is convex. A small notch is present
365 where the anterolateral portion of the maxilla meets the palatal process. This notch is similar to
366 that of *Batrachotomus kuperferzellensis* (SMNS 52970), *Saurosuchus galilei* (PVSJ 32),
367 *Fasolasuchus tenax* (PVL 3851), and *Postosuchus kirkpatricki* (TTUP 9000). In these taxa, a
368 foramen is formed between the articulation of the premaxilla and maxilla when in articulation;
369 this morphology was heavily discussed by Gower (2000) and Nesbitt (2011). *Heptasuchus clarki*
370 was originally reported (Dawley et al. 1979) to have an elongated fenestra between the maxilla
371 and premaxilla similar to what was reported in *Saurosuchus galilei* (PVL 2062; Reig 1959) and
372 *Luperosuchus fractus* (PULR 04; Romer 1971). However, it appears that these elongate
373 fenestrae are the result of disarticulation or deformation (see Nesbitt 2011; Nesbitt and Desojo
374 2018). Therefore, the elongated fenestra reconstructed in *Heptasuchus clarki* (Fig. 2 of Dawley
375 et al. 1979) is likely not present. An anteriorly opening foramen is present within the notch
376 between the lateral side of the maxilla and the palatal process which is also found in
377 *Postosuchus kirkpatricki* (Weinbaum (2011). Another, smaller anteriorly opening foramen is
378 located just posterodorsal to the foramen in the notch. The transition between the lateral side of
379 the maxilla and the palatal process is continuous as in *Postosuchus kirkpatricki* (TTUP 9000)
380 and *Fasolasuchus tenax* (PVL 3851), a condition in contrast to *Batrachotomus kuperferzellensis*
381 (SMNS 52970) where there is a distinct step. There is no clear facet on the anterodorsal surface
382 of the maxilla for the posterodorsal process of the premaxilla. Here, the surface is incompletely
383 preserved but appears to be concave in lateral view between the palatal process and the base
384 of the dorsal process, as in *Batrachotomus kuperferzellensis* (SMNS 52970). It is unknown if the
385 mediolaterally compressed ridge of bone that forms the anterodorsal margin of the maxilla
386 contributed to the border of the external naris as it does in *Batrachotomus kuperferzellensis*
387 (Gower 1999). The base of the dorsal process is oval in cross-section similar to what is present
388 in *Batrachotomus kuperferzellensis* (SMNS 52970) and *Arizonasaurus babbitti* (MSM 4590)

389 rather than the anteroposteriorly elongated cross-sections of taxa such as *Postosuchus*
390 *kirkpatricki* (TTUP 9000).
391 The entire lateral side of the maxilla ventral to the antorbital fossa is covered in small
392 ridges and shallow grooves much like that in the holotype of *Saurosuchus galilei* (PVL 2062). A
393 slight bank marks the division of the antorbital fossa from the main body of the maxilla as in
394 *Fasolasuchus tenax* (PVL 3851), *Batrachotomus kuperferzellensis* (SMNS 52970), and
395 *Saurosuchus galilei* (PVSJ 32) and not separated by a distinct step as in *Polonosuchus*
396 *silesiacus* (ZPAL Ab III/563) and *Postosuchus kirkpatricki* (TTUP 9000). The depth of the
397 antorbital fossa deepens posteriorly in *Heptasuchus clarki* as well as *Fasolasuchus tenax* (PVL
398 3851), *Batrachotomus kuperferzellensis* (SMNS 52970), *Saurosuchus galilei* (PVSJ 32), a
399 specimen referred to *Prestosuchus* (UFRGS-PV 156 T), and in the crocodylomorph
400 *Dromicosuchus grallator* (NCSM 13733). The posterior portion of the maxilla expands dorsally
401 as in *Turfanosuchus dabanensis* (IVPP V33237) and gracilisuchids unlike most loricatans. The
402 bone that forms the antorbital fossa is thin posteriorly as in *Postosuchus kirkpatricki* (TTUP
403 9000), *Fasolasuchus tenax* (PVL 3851), and *Batrachotomus kuperferzellensis* (SMNS 52970)
404 and other archosaurs (e.g., *Xilousuchus sapingensis,* IVPP V6026). The tooth bearing ventral
405 margin is convex for the length of the element as in *Batrachotomus kuperferzellensis* (SMNS
406 52970).
407 The first alveolus is the smallest in the maxilla as typical for taxa classically grouped as
408 “rauisuchians” (Brusatte et al. 2009). The alveoli increase in size posteriorly to the fourth and
409 fifth alveolus then gradually decrease in size posteriorly based on our reconstructed maxilla
410 from the two pieces. The outline of all the alveoli is ovate in ventral view.
411 In medial view, a step separates the medial surface of the maxilla from the interdental
412 plates. The step in horizontally oriented and extends the length of the preserved section of
413 maxilla. Anteriorly, the step is located in the dorsoventral middle of the body of the maxilla as in
414 *Fasolasuchus tenax* (PVL 3851) and *Batrachotomus kuperferzellensis* (SMNS 52970) whereas

415 the step is located in the ventral third of the anteromedial surface of the maxilla of *Postosuchus*
416 *kirkpatricki* (TTUP 9000). The anteriormost portion of the step disappears posterior to the
417 anterior termination of the maxilla in *Heptasuchus clarki*. The palatal process is horizontally
418 oriented at the anterodorsal portion of the maxilla. The process is thin dorsoventrally as in
419 *Fasolasuchus tenax* (PVL 3851) and *Batrachotomus kuperferzellensis* (SMNS 52970) whereas
420 the process is dorsoventrally deeper in *Postosuchus kirkpatricki* (TTUP 9000). A distinct fossa
421 on the ventral surface of the maxilla is present in *Heptasuchus clarki*. Recently, this character
422 state (see character 426 in the appendix) was hypothesized to be an autapomorphy of
423 *Postosuchus kirkpatricki* by Weinbaum (2011), a deep fossa on the ventral surface of the palatal
424 process is also present in *Polonosuchus silesiacus* (ZPAL Ab/III 563), *Fasolasuchus tenax* (PVL
425 3851), *Batrachotomus kuperferzellensis* (SMNS 52970), and the crocodylomorph
426 *Sphenosuchus acutus* (SAM 3014), but absent in *Saurosuchus* (PVSJ 32) and poposauroids
427 (e.g., *Xilousuchus sapingensis*). Along the ventral half of the medial surface of the tooth row, the
428 internal walls of the alveoli are formed by fused interdental plates at least anteriorly. The
429 interdental plates of all *Batrachotomus kuperferzellensis* (e.g., SMNS 52970) specimens are
430 unfused whereas the interdental plates of *Postosuchus kirkpatricki* (TTUP 9000) and
431 *Teratosaurus suevicus* (NHMUK 38646) are completely fused together. The loss of the medial
432 surface on the posterior half of the maxilla has exposed the tips of replacement teeth medial to
433 the roots of the fully erupted teeth. Posteriorly, the maxilla separates into two portions, a ventral
434 portion that houses the alveoli and a mediolaterally thin dorsal portion. The ventral portion
435 tapers posteroventrally and expands more posteriorly than the thin dorsal portion. A posteriorly
436 opening foramen lies at the juncture of the ventral and dorsal portions. Here, a faint facet for the
437 articulation with the jugal can be followed posteriorly on the dorsal surface of the maxilla.
438
439 **Jugal:** Both the right and left jugals of *Heptasuchus clarki* are represented in the holotype (UW
440 ll562-D and -E, respectively; Fig. 5D-F). The right jugal is missing the dorsal end of the

441 ascending process and the posterior portion of the posterior process whereas the left element is
442 missing much of the posterior process. The jugal is a triradiate structure, with two dorsal
443 processes contributing to the ventral portions of the anterior and posterior walls of the orbit and
444 a posterior process forming much of the lower margin of the infratemporal fenestra. The
445 anterodorsal process projects forward at approximately 50° anterodorsally along its contact with
446 the maxilla. Elongated groove and ridges mark the articulation with the maxilla and this
447 articulation terminates posteriorly in an acute angle within the body of the jugal. A similar
448 termination within the jugal is present in *Batrachotomus kuperferzellensis* (SMNS 52970) as well
449 as *Revueltosaurus callenderi* (PEFO 34561) and aetosaurs (Nesbitt 2011). The anterodorsal
450 process mediolaterally in the dorsal direction where it would meet the lacrimal. The articulation
451 surfaces with the maxilla and the lacrimal are separated by a distinct anteroposteriorly trending
452 ridge that continues posteriorly as the laterally expanded jugal ridge. Anteriorly, this ridge is
453 sharp, mediolaterally thin, hides parts of the lateral side of jugal in lateral view, and dorsally
454 forms a small shelf. A similar shelf is present in *Batrachotomus kuperferzellensis* (SMNS 52970)
455 and clearly absent in *Postosuchus kirkpatricki* (TTUP 9000) and *Saurosuchus galilei* (PVSJ 32).
456 The anterior surface shifts vertically at the anterior edge, and terminates in a sutural surface
457 with the lacrimal. The lacrimal appears to have articulated with the lateral side of the jugal but
458 the details of this articulation are not clear.
459 The large jugal ridge on the lateral side of the body of the jugal of *Heptasuchus clarki*
460 continues for the length of the jugal. The lateral side of the ridge is covered in small
461 anteroposteriorly trending ridges and lacks the long grooves present in *Batrachotomus*
462 *kuperferzellensis* (SMNS 52970). In its anteroposterior center, the lateral ridge is asymmetrical
463 where the dorsal portion is more laterally expanded then the ventral portion. This asymmetry is
464 also present *Batrachotomus kuperferzellensis* (SMNS 52970) whereas other
465 paracrocodylomorphs (e.g., *Postosuchus kirkpatricki*, *Saurosuchus galilei*) have a dorsoventrally

466 symmetrical lateral ridge. The posterior process is rectangular in cross-section and the ventral
467 edge of the jugal is nearly straight.
468 The dorsal process of the jugal arcs posterodorsally at it dorsal termination. The lateral
469 side bears a shallow fossa at the base and on the posterior half of the process. A similar fossa
470 is also present in *Batrachotomus kuperferzellensis* (SMNS 52970). The anterior edge of the
471 dorsal process is mediolaterally thin and distinctly convex as in *Batrachotomus kuperferzellensis*
472 (SMNS 52970) whereas the anterior edge is typically straight in other loricatans (e.g.,
473 *Postosuchus kirkpatricki*; TTUP 9000). The anterior bowing of the anterior edge of the dorsal
474 process of *Heptasuchus clarki* suggests that the ventral portion of the orbit is more
475 anteroposterior restricted than the dorsal portion of the orbit. Therefore, it is clear that
476 *Heptasuchus clarki* had a 'keyhole shaped' (sensu Benton and Clark 1988) orbit as with non-
477 crocodylomorph loricatans and other large carnivorous archosaurs (e.g., allosaurids,
478 tyrannosaurids). In *Heptasuchus clarki*, the thin anterior margin hides the articular surface with
479 the postorbital. The concave posterior margin of the process is mediolaterally thin and overall,
480 the dorsal process is subcircular in cross-section at its base.
481 Medially, the body of the jugal is convex anteriorly and concave posteriorly. The
482 posterior process bears an anteroposteriorly oriented groove that is also present in the
483 loricatans *Batrachotomus kuperferzellensis* (SMNS 52970), *Postosuchus kirkpatricki* (TTUP
484 9000), some crocodylomorphs (e.g., *Sphenosuchus acutus*, Walker 1990) and in phytosaurs
485 (Stocker 2010; Stocker and Butler 2013). Anteriorly, just ventral to the dorsal process, the
486 groove divides the articular facets for the ectopterygoid. The head of the ectopterygoid likely
487 split into two lateral heads as with *Batrachotomus kuperferzellensis* (SMNS 80260),
488 *Postosuchus kirkpatricki* (Weinbaum 2011), and crocodylomorphs (e.g., *Sphenosuchus acutus*,
489 Walker 1990). The dorsal articular surface for the ectopterygoid is round and poorly defined
490 whereas the ventral articulation is well defined and extends to the ventral edge of the jugal. The
491 articular surface with the postorbital lies on the anteromedial edge of the dorsal process and

492 extends ventrally for much of the length of the dorsal process. Therefore, the anterior edge is
493 mediolaterally thick. Anteriorly, the jugal has a shallow fossa on the ventral edge, opposite the
494 articular facets. A small channel is present between the fossa and the ventral articular surface
495 with the ectopterygoid.
496
497 **Nasal:** A nearly complete right nasal (UW ll562-F) is known for *Heptasuchus clarki* (Fig. 4G-H);
498 only the anterior portion that meets the anterodorsal (=nasal) process of the premaxilla is
499 missing. The nasal formed the posterodorsal portion of the external nares. The anterior half of
500 the nasal divides into a robust anterior process that would have met the anterodorsal process of
501 the premaxilla, if complete, and a shorter, anteroventrally directed process that lies on the
502 anterodorsal margin of the maxilla. The anterior process bows dorsally to form a “roman nose”
503 similar to that of *Batrachotomus kuperferzellensis* (Gower 1999), *Saurosuchus galilei* (PVSJ
504 32), a skull assigned to *Prestosuchus chiniquensis* (UFRGS T-156), *Luperosuchus fractus*
505 (PULR 04; Nesbitt and Desojo 2018), and *Decuriasuchus quartacolonia* (França et al. 2011).
506 The lateral surface of the anterior process bears a rugose lateral ridge that continues posteriorly
507 to the articular surface with the lacrimal. This ridge is similar to that in *Postosuchus kirkpatricki*
508 (TTUP 9000) and *Batrachotomus kuperferzellensis* (Gower 1999). A distinct fossa is present
509 posterodorsal to the external naris at the junction of the anterior process and the anteroventral
510 process. The fossa is well defined is similar to that of *Batrachotomus kuperferzellensis* (Gower
511 1999) (see character 430) and an isolated nasal fragment (NMMNH 55779) from the Middle
512 Triassic Moenkopi Formation of New Mexico (Schoch et al. 2010). The anteroventral process
513 tapers just ventral to the posterior extent of the external naris. The location of the anterior
514 termination of this process is not known and it is not clear if the process met the posterodorsal
515 process of the premaxilla, hence excluding the maxilla from the external naris, as in the case in
516 *Batrachotomus kuperferzellensis* (Gower 1999).

517 The nasal articular surfaces with the maxilla and lacrimal lie at the ventrolateral edge
518 and are oriented almost vertically, indicating a nearly perpendicular contact between these
519 bones and the nasal. It appears that the nasal formed the anterodorsal portion of the antorbital
520 fossa in *Heptasuchus clarki* as in *Batrachotomus kuperferzellensis* (Gower 1999) but not in
521 *Postosuchus kirkpatricki* (TTUP 9000) or *Saurosuchus galilei* (PVSJ 32). Dorsally, the surface
522 medial to the lateral ridge is dorsoventrally thin and concave at the midline like that of
523 *Postosuchus kirkpatricki* (TTUP 9000), *Batrachotomus kuperferzellensis* (Gower 1999), the
524 crocodylomorph *Sphenosuchus acutus* (Walker 1990) and *Turfanosuchus dabanensis* (IVPP
525 V3237). This concave depression narrows anteriorly until it disappears just posterior to the
526 division of the anterior portion of the nasal.
527 The medial surface of the nasal bears a dorsoventrally thick midline suture that thins
528 posteriorly. The suture itself bearsa a series of complex grooves and ridges. The medial surface
529 is largely concave anteriorly and flat posteriorly where the nasal is dorsoventrally thin.
530
531 **Skull roof elements:** A large fragment of the skull roof (UW ll562-G) comprises the right
532 prefrontal, postfrontal, frontal, and postorbital (Fig. 5A-C). With the exception of the frontal, the
533 elements are essentially complete, but microfracturing has obscured the sutural contacts
534 between them.
535 The prefrontal (Fig. 5C) lies on the anterolateral edge of the frontal and forms the
536 anterodorsal corner of the orbit. The lateral margin bears a rugose lateral ridge that could have
537 been continued from the nasal to the lacrimal to the prefrontal. The posterolateral margin of the
538 prefrontal does not have a clear sutural contact for a supraorbital element or palpebral(s) that
539 are present on the prefrontal in *Saurosuchus galilei* (PVSJ 32) and *Postosuchus kirkpatricki*
540 (TTUP 9000; Nesbitt et al. 2013b). A rugose articulation with the lacrimal located on the anterior
541 portion prefrontal is inset from the lateral margin and rounded posteriorly. The ventral end of the
542 prefrontal is broken.

543 The frontal is incomplete anteriorly and medially. The frontal clearly contributes to the
544 lateral margin of the orbit. Here, the lateral orbital margin is rounded and slightly rugose. The
545 preserved portion of the dorsal surface of the frontal is smooth, but much of the surface is poorly
546 preserved and fragmented. The suture between the postfrontal and the frontal is clear on the
547 ventral surface of the elements. Posteriorly, it appears that the part of the supratemporal fossa
548 is present on the frontal as in crocodylomorphs, dinosaurs, and *Batrachotomus*
549 *kuperferzellensis* (SMNS 80260) (Nesbitt 2011). In *Postosuchus kirkpatricki* (TTUP 9000), a
550 supratemporal fossa is present anterior to the supratemporal fenestra, but present only on the
551 postfrontal (Nesbitt 2011). Thus, among non-crocodylomorph loricatans, a fossa on the
552 posterior portion of the frontal seems to be restricted to *Heptasuchus clarki* and *Batrachotomus*
553 *kuperferzellensis*. The posterior edge of the frontal contributes to the supratemporal fenestra.
554 The postfrontal lies at the posterodorsal edge of the orbit. In dorsal view, the
555 anterolateral corner angle is nearly 90° from the anterior orbital margin to the lateral margin. The
556 anterior and the lateral edges of the element are rounded and have small grooves on them. The
557 body of the postfrontal dorsally overhangs the postorbital where the two elements meet. The
558 medial portion tapers posteromedially between the frontal and the postorbital and apparently, is
559 not part of the supratemporal fossa.
560 The postorbital is nearly completely preserved. The postorbital has two components, a
561 dorsal portion, which forms part of the skull table and a ventrally process, which separates the
562 orbit and infratemporal fenestra. The dorsal portion is a flat, mediolaterally expanded element
563 which forms the lateral portion of the supratemporal fenestra. The medial side of the postorbital
564 bears a supratemporal fossa that is continuous with the fossa of the frontal. This is also present
565 in *Batrachotomus kuperferzellensis* (SMNS 80260), but absent in other loricatans examined
566 here. The fossa shallows posteriorly and disappears at the posterior portion. A posterolaterally
567 directed ridge originates at the border of the supratemporal fenestra and crosses the postorbital
568 to terminate on the lateral edge of both *Heptasuchus clarki* and *Batrachotomus*

569 *kuperferzellensis* (SMNS 80260). The posterior portion of the postorbitals of *Heptasuchus clarki,*
570 *Batrachotomus kuperferzellensis* (SMNS 80260), and *Postosuchus kirkpatricki* (TTUP 9000) are
571 relateively wider than that of *Saurosuchus galilei* (PVSJ 32), a skull assigned to *Prestosuchus*
572 *chiniquensis* (UFRGS T-156), and *Luperosuchus fractus* (UNLR 04). The posterior portion of the
573 postorbital of *Heptasuchus clarki* appears to overlay the squamosal as in *Batrachotomus*
574 *kuperferzellensis* (SMNS 80260), and *Postosuchus kirkpatricki* (TTUP 9000) (see character
575 428).
576 The laterally oriented, rugose ridge continues from the postfrontal to the postorbital. The
577 ridge splits into ventral and posterior components with a small gap on the anterior side where
578 the ridges come together. The ventral ridge forms the posterior margin of the orbit for the length
579 of the ventral process. Directed ventrally at its origin, the ridge, along with the ventral process,
580 curves gradually anteroventrally describing an arc of nearly 50°. The ridge is rugose and similar
581 to that of *Batrachotomus kuperferzellensis* (SMNS 80260) although the degree of rugosity
582 differs among *Batrachotomus kuperferzellensis* individuals (SMNS 80260 versus SMNS 52970).
583 Posterior to the dorsal portion of the ridge, a large fossa is present that is roofed by the dorsal
584 portion of the postorbital. This deep fossa is also present in *Batrachotomus kuperferzellensis*
585 (SMNS 80260) and also, to a lesser degree in *Saurosuchus galilei* (PVSJ 32), a skull assigned
586 to *Prestosuchus chiniquensis* (UFRGS T-156), and *Postosuchus kirkpatricki* (TTUP 9000). The
587 ridge terminates dorsoventrally in a broad flange that clearly entered the orbit and contributed to
588 the ‘keyhole shape’ of the orbit. Additionally, a deep fossa is present on the anterodorsal side of
589 the ventral termination of the postorbital. This deep fossa, which extends dorsally into the
590 ventral process, is only visible in anterior view. A similar feature is also present in
591 *Batrachotomus kuperferzellensis* (SMNS 80260) and was originally considered to be an
592 autapomorphy of the taxon by Gower (1999) (see character 428). However, the fossa in
593 *Batrachotomus kuperferzellensis* is located only on the lateral surface whereas the feature in
594 *Heptasuchus clarki* is only on the anterodorsal surface. It is not clear if this difference is the

result of crushing in *Heptasuchus clarki*. Moreover, the depth of the fossa differs among *Batrachotomus kuperferzellensis* individuals (SMNS 80260 versus SMNS 52970).

The ventral process of the postorbital is subrectangular in cross-section for the length of the element. The ventral process lacks the 'kink' as in *Batrachotomus kuperferzellensis* (SMNS 80260), *Postosuchus kirkpatricki* (TTUP 9000), and *Saurosuchus galilei* (PVSJ 32). However, this 'kink' is subtle in taxa with the feature and may be difficult to detect if parts of the posteroventral margin of the ventral process are incomplete. In medial view, a shallow and broad groove posterior to a ridge on the anterior edge of the ventral process marks the articulation with the dorsal process of the jugal. The articular surface with the jugal is restricted to the posteroventral side of the ventral process. A shallow fossa is present at the dorsal margin of the ventral process and may represent the articular surface with the laterosphenoid.

Parietal: Only the lateral portion of the occipital process is preserved (Fig. 6). The process remains in articulation with the supraoccipital and possibly touches the paroccipital process posterior laterally. The vertically oriented process forms the dorsal portion of a large post temporal fenestra. A distinct ridge is present on the anterior side of the lateral process.

Occiput and Braincase: The three dimensionally preserved braincase (UW ll562-H) is largely complete on the right side and preserves the opisthotic, exoccipital, occipital and parabasisphenoid, prootic, and the right half of the supraoccipital (Fig. 6). The bone surface is well preserved and details of the morphology of the medial surfaces are readily apparent. The braincase is well ossified and sutures between most elements cannot be distinguished in most cases.

The basioccipital forms the majority of the occipital condyle and the exoccipitals are completely fused to the dorsolateral surfaces. A small notochordal pit is present on the dorsal portion of the basioccipital. The condylar stalk (=neck) is well expanded and a distinct rim

621 outlines the circumference of the basioccipital. The preserved portion of the foramen magnum is
622 semicircular in shape and its flattened floor extends onto the dorsal surface of the occipital
623 condyle. The basitubera originate at the ventral portion of occipital condyle and stretch
624 ventrolaterally. As with *Batrachotomus kuperferzellensis* (SMNS 80260), the basitubera are
625 bilobed and are separated from the basitubera of the parabasisphenoid by an unossified gap.
626 The unossified gap of *Heptasuchus clarki* is large like that of *Saurosuchus galilei* (PVSJ 32).
627 The lateral edge of the more lateral lobe of the basitubera is continuous with the lateral ridge
628 (sensu Gower 2002) that originates on the exoccipital. The more medial lobe of *Heptasuchus*
629 *clarki* is larger and is distinctly convex in contrast to that of the basitubera of *Postosuchus*
630 *kirkpatricki* (TTUP 9000). There is no division between the basioccipital and the
631 parabasisphenoid at the midline.
632 Only the right exoccipital is fully preserved. The exoccipitals meet on the midline
633 similarly to most pseudosuchians other than crocodylomorphs and shuvosaurids (Nesbitt 2011).
634 The lateral side of the exoccipital bears a lateral ridge that obstructs the descending process of
635 the opisthotic in posterior view similar to that of *Batrachotomus kuperferzellensis* (SMNS
636 80260), *Postosuchus kirkpatricki* (Weinbaum 2011), crocodylomorphs and aetosaurs (Gower
637 and Walker 2002). Two foramina, interpreted as the exits of cranial nerve XII, pierce the medial
638 surface of the exoccipital. However, only one exit cranial nerve XII can be observed on the
639 lateral side of the exoccipital. This exit is located anterior to the lateral ridge and directed into
640 the opening for the metotic opening as with *Batrachotomus kuperferzellensis* (Gower 2002). The
641 opisthotic is fused with the exoccipital.
642 The well-preserved prootic, which separates the parabasisphenoid from the
643 laterosphenoid is complete, however, the sutures with the surrounding elements are difficult to
644 discern. The anterolateral surface bears the exits for cranial nerves V and VII. The exit for
645 cranial nerve V appears to lie completely within the prootic as in *Postosuchus kirkpatricki*
646 (Weinbaum 2011) and not shared with the laterosphenoid as in *Batrachotomus*

kuperferzellensis (Gower 2002) and *Sphenosuchus acutus* (Walker 1990). A fossa surrounds the opening for cranial nerve V in *Heptasuchus clarki*. Anteriorly, a groove is present linking the exit for cranial nerve V and the anterior edge. A notch on the anterodorsal edge, just anteromedial to the exit of cranial nerve V, possibly represents the exit middle cerebral vein. A slight groove leads anteriorly into the notch. A small ridge located dorsal to the exit of cranial nerve V is interpreted to be the site of attachment for the protractor pterygoidei following Gower and Sennikov (1996) and Gower (2002). There is a vertical ridge on the small anterior portion of the prootic just anteroventral to the exit of cranial nerve V. The pathway of cranial nerve IV appears to pierce the anterior, upturned process of the prootic. This process separates the laterosphenoid from the parabasisphenoid.

The exit for cranial nerve VII is located in a posterolaterally opening slot on the posterolateral portion of the prootic. The deep pocket for the exit of cranial nerve VII continues ventrally as a groove on the lateral on the lateral side of the parabasisphenoid. The surface between the exits of cranial nerves V and VII is concave. There is no contact between the anterolateral surface of the prootic and the quadrate as in crocodylomorphs (Gower 2002).

Medially, the surface of the prootic is not well preserved. There is no clear pneumatization of inner ear as in crocodylomorphs as described by Walker (1990). The medial wall of vestibule appears to be nearly fully ossified as with most suchians (Gower 2002; Gower and Nesbitt 2006), but the center of the wall is broken.

The right opisthotic is completely preserved. The stapedial groove leading into the fenestra ovalis is shallow and poorly defined anteriorly. The descending process of the opisthotic (=crista interfenestralis) divides the metotic foramen anteriorly from the fenestra ovalis posteriorly. This thin process of the opisthotic is expanded mediolaterally. Nearly all of the descending process of the opisthotic is hidden posteriorly by the lateral ridge on the exoccipital in *Heptasuchus clarki* as in aetosaurs, *Batrachotomus kuperferzellensis, Postosuchus kirkpatricki,* and crocodylomorphs (Gower 2002). There does not appear to be a foramen in the

673 dorsal portion of the metotic opening as there is in *Batrachotomus kuperferzellensis* (Gower
674 2002), but this area is incompletely prepared. The perilymphatic foramen is not fully ossified but
675 must have been oriented posteriorly and not laterally as in *Sphenosuchus acutus* (Walker 1990)
676 and other crocodylomorphs (Gower 2002).
677 Lateral to the foramen magnum, the paroccipital processes of the opisthotics, are
678 constricted (to 2.3 cm) at their bases but broaden considerably (to 5.2 cm) to form club-shaped
679 posterolateral expansions. The processes are directed dorsolaterally at an angle of 35° from the
680 vertical plane of the occiput. The broadness of the lateral portions of the paroccipital processes
681 is greater than that of *Batrachotomus kuperferzellensis* (SMNS 80260), but similar to
682 *Postosuchus kirkpatricki* (Weinbaum 2011) and crocodylomorphs (e.g., *Sphenosuchus acutus*).
683 The ventral portion of the process of *Heptasuchus clarki* is nearly straight whereas the dorsal
684 margin is significantly expanded dorsally. The dorsal edge of the process forms the ventral
685 margin of a clear post temporal fenestra. Shallow grooves are present on the ventral surface of
686 the paroccipital process. The lateral edge of the paroccipital is rounded like that of
687 *Batrachotomus kuperferzellensis* (SMNS 80260).
688 The basisphenoid and parasphenoid are fused together to form a parabasisphenoid. The
689 body of the parabasisphenoid is vertically oriented where the basipterygoid processes are
690 extended well ventral of the basitubera. The parabasisphenoid portion of the basitubera project
691 laterally and dorsolaterally at its tips. A deep fossa (=medial pharyngeal recess, =hemispherical
692 fontanel) is positioned between the basitubera and the midline. This depression is undivided on
693 the midline whereas there is a distinct lamina of bone dividing the depression in *Batrachotomus*
694 *kuperferzellensis* (Gower 2002) and *Sphenosuchus acutus* (Walker 1990). There is no interbural
695 plate (Gower and Sennikov 1996) across the midline. The body of the parabasisphenoid is
696 waisted between the basitubera and the basipterygoid processes. The posteriorly directed
697 basipterygoid processes extend ventrally beyond the rest of the braincase. The articular
698 surfaces with the pterygoid are positioned on the anterior portion of the basipterygoid

699 processes. The posterior portions of the processes expand posterodorsally into mediolaterally
700 thin sheets of bone. These processes are autapomorphic (see diagnosis) for *Heptasuchus clarki*
701 and represent a clear difference between *Heptasuchus clarki* and *Batrachotomus*
702 *kuperferzellensis*.
703 Laterally, the entrance of the internal carotid arteries lies in the groove that is continued
704 from the prootic on the lateral side of the parabasisphenoid. The path of the internal carotid
705 travels anteriorly to exit at the base of the hypophyseal fossa as observed on the broken left
706 lateral side. The articulation of the descending process of the opisthotic with the
707 parabasisphenoid is not distinct. The base of both the metotic fenestra and the fenestra ovalis
708 are broadly rounded and lie on the dorsal portion of the parabasisphenoid. The ventral base of
709 the metotic is well ventral to the contact between the basioccipital and the exoccipital.
710 The cultriform process is complete, relatively short compared with the braincase, and
711 dorsoventrally expanded posterior to the anteriorly tapering tip. A dorsoventrally expanded
712 cultriform process is also present in *Batrachotomus kuperferzellensis* (Gower 2002) and
713 *Postosuchus kirkpatricki* (Weinbaum 2011). A distinct ventral step is present in the anterior half
714 of the element. There does not appear to be a longitudinal groove on the dorsally surface of the
715 cultriform process as in *Arizonasaurus babbitti* (Gower and Nesbitt 2006). Comparisons with the
716 length and dorsoventral depth of the cultriform process are limited among suchians given this
717 region is not common preserved.
718 Dorsal to the foramen magnum, the vertically inclined face of the supraoccipital extends
719 dorsally to contact the parietal. The auricular recess does not appear to extend onto the
720 supraoccipital.
721
722 **Quadrate:** The dorsal (UW 11563-AD) and ventral portions (UW 11563-AF, UW 11563-H) of
723 the left quadrate were found among the weathered elements collected at the locality. The dorsal
724 fragment (Fig. 7D) that articulated with the squamosal, is rounded in dorsal view, and the

surface is composed of spongy bone circumscribed by a ring of compacta bone. There is no posterior hook of the quadrate as there is in *Postosuchus kirkpatricki* (TTUP 9000). The ventral portion consists of the articular facet with the articular (Fig. 7A-C). The convex facet is divided into medial and lateral condyles separated by a shallow fossa. The more medial condyle of the articular surface projects further ventrally. The ventral articular surfaces lap dorsally onto the anterior surface. Anteriorly, a small but well-defined ridge originated on the lateral condyle and trends dorsomedially.

Palate: A nearly complete left palatine (UW ll562-K, Fig. 5F) is the only confirmed (see below) portion of the palate represented in the type specimen. The thin medial, anterior and posterior portions of the element are incomplete. The body of the palatine is thin for nearly the length of the element. The lateral side bears a dorsoventrally expanded, anteroposteriorly straight facet for articulation with the medial side of the maxilla. In dorsal view, the expansion forms a lateral lip on the lateral side of the element. The posterolateral portion forms the anteromedial margin of the suborbital fenestra and the posterior portion tapers posteromedially. Anteriorly, only a portion of the dorsal fossa that holds the pterygoideus muscle (Witmer 1997) is preserved. The portion preserved suggests that the fossa is anteriorly shifted near the choana as in *Batrachotomus kuperferzellensis* (Gower 2002) relative to the more posterior position in *Polonosuchus silesiacus* (ZPAL Ab/III 563), *Saurosuchus galilei* (PVSJ 32), aetosaurs (Gower and Walker 2002), and the crocodylomorph *Sphenosuchus acutus* (Walker 1990). The posterior border of the choana is thickened relative to the body in *Heptasuchus clarki* but does not possess a surrounding rim in the same area as in *Polonosuchus silesiacus* (ZPAL Ab/III 563). Ventrally, the surface is nearly flat except for a shallow facet for the articulation with the pterygoid on the posteromedial portion.

Dentition: A single premaxillary tooth (UW ll562-A), the first five teeth of the left maxilla (UW ll562-C) and the fourth, sixth, and ninth tooth of the right maxilla (UW ll562-) are preserved in place in the holotype (Fig. 4). Loose teeth (UW ll562-AA through -AI) found at the locality are referred to *Heptasuchus clarki* based on similarity, but only the teeth found in the tooth bearing bones are described in detail. The roots of the premaxillary and maxillary teeth lie in deep sockets.

The only preserved premaxillary tooth, in either tooth position two or three (Fig. 4E-F), is unique in its morphology in that the proximal half of the crown is cylindrical in shape and bears no serrations. The tip grades into a distal portion, which is compressed to form a blade similar in shape to the distal tips of the maxillary teeth. The axis of this blade, however, lies at an angle to the blade axis of the maxillary teeth.

Generally, the maxillary teeth are ziphodont in that they mediolaterally compressed, recurved, and bear serrations on the mesial and distal sides. The crowns are long, that of a fully erupted tooth being approximately equal in length to its root. Typically, there are 12 serrations per 5 mm. The left maxilla (Fig. 4A-B), bearing the first five teeth of the maxillary series, clearly shows the pattern of tooth replacement. As in *Saurosuchus galilei* (Sill 1974), the teeth grow and are replaced in two alternating waves. Teeth in positions three and five were newly erupted when the individual was buried whereas teeth in positions two and four are fully erupted. Tooth position two shows especially severe signs of wear, as its tip is badly blunted and the serrations were worn away, likely in life. The right maxilla (Fig. 4C-D), with the medial wall almost entirely removed by erosion, illustrates the process of tooth replacement in *Heptasuchus clarki*; tooth position six is fully erupted and a replacement tooth lies on its lingual surface within a socket of the fully erupted tooth at the base of its root.

Pterygoid: Two elements (UW 11562-L and UW 11562-M; Fig. 7E-H) not readily identified originally were found in situ with the holotype; here we interpret these fragments as parts of the

776 pterygoid. UW 11562-L consists of a thin, plate like element that is possibly part of the lateral
777 process of the pterygoid. All sides except one, presumably the medial side, are broken. The
778 'medial' side is straight with a distinct step at the edge near the middle of the element. Here the
779 bone is rugose and may serve an articular facet. The nearly flat surfaces are nearly featureless.
780 UW 11562-M is a thin fragment that may pertain to the anterior (=palatine) process of the
781 pterygoid. The element likely tapers anteriorly and between longitudinal ridges on both sides.
782
783 **Postcranial Skeleton**
784 The postcranial of *Heptasuchus clarki* is only represented by a few complete or nearly
785 complete bones (e.g., pubis, tibia, ulna) whereas most other postcranial elements were either
786 found on the surface after extensive surface weathering. It is apparent that much of the shaft of
787 limb bones and delicate parts of vertebrae (e.g., base of the neural arches) were weathered
788 away much easier than the more robust elements, such as limb bone ends and centra
789 fragments. A few postcranial bones were found in place (e.g., trunk vertebra; Fig. 8A-B), but
790 suffer from poor surface details with few exceptions.
791
792 **Vertebrae:** The vertebral column of *H. clarki* is represented by only a few poorly preserved
793 centra, one complete neural spine, and a large number of fragments from neural arches (e.g.,
794 diapophyses from trunk vertebrae) along the column. Those centra sufficiently preserved to
795 warrant description include parts of three cervicals, a trunk, and parts of caudal centra.
796 The most anterior vertebra represented among the referred material consists of a
797 fragmentary centrum (UW ll562-T) from approximately the middle of the cervical series
798 (comparing to that of *Postosuchus kirkpatricki* Weinbaum 2013) which retains the anterior and
799 posterior articular surfaces and the length of this centum is a bit less than its height, typical of
800 loricatan taxa with short necks (e.g., *Batrachotomus kupferzellensis*, Gower and Schoch 2009;
801 *Postosuchus alisonae,* Peyer et al., 2008; *Prestosuchus chiniquensis*, Desojo et al. 2020).

Between the articular faces, the centrum is constricted in ventral view. Lateral to the anterior articular facet, the parapophyses sit on the ventral half of the centrum and project laterally. They are separated by a ventrally projecting lip, which originates from the ventral portion of the anterior facet. The ventral surface of the centrum bears a slight ridge (=keel), as typical of most archosauriforms (Nesbitt 2011).

The a more posterior cervical centrum is represented by just the anterior portion (UW ll564-A). The anterior articular facet is circular and only shallowly concave. Lateral to the anterior articular facet, the parapophyses lie slightly more dorsally on the centrum than in UW ll562-T. The parapophyses face laterally with a slight posterior component. Just posterior to anterior articular facet, the centrum constricts rapidly to the point where it has broken, preserving only about half of the total length of the element based on our estimation and comparisons to *Batrachotomus kupferzellensis* (Gower and Schoch 2009) and *Postosuchus alisonae* (Peyer et al., 2008). The marked constriction decreases width from 4.5 cm at the anterior articular facet rim to l.5 cm at the midpoint. A trace of a faint ridge (=keel) is present on the midline of the ventral surface. In this vertebra, as in all those preserved in *Heptasuchus clarki*, the neural canal deeply indents the dorsal portion of the body of the centrum behind the flared rim. This condition "central excavation" is present in archosauriforms outside crown Archosauria *Euparkeria capensis* (Ewer l965), and also with the crown (e.g., *Arizonasaurus babbitti*, Nesbitt 2005).

Much of a centrum of a trunk vertebra (TMM unnumbered; Fig. 8A-B) was excavated from the ground in 2009, but the specimen is poorly preserved and lacks the process of the neural arch. TMM unnumbered likely represents a mid to posterior trunk vertebra based on the dorsal and posteriorly placed parapophysis based on comparison with other loricatans (e.g., *Batrachotomus kupferzellensis*, Gower and Schoch 2009). The anterior and posterior articular facets of the centrum are circular with a slightly dorsoventral height compared to the mediolateral width. The centrum rims are well pronounced, but slightly weathered, and the

centrum is well constricted in both lateral and ventral views between that articular facets. The neurocentral suture is fused and no trace can be observed. The lateral portions of the diapophyses are broken, but the base is shifted posteriorly and likely connected with the base of the diapophyses. Posteriorly, the neural canal oval with a much greater height dorsoventrally than mediolateral width. This height to width ratio of 0.7 in *Heptasuchus clarki* is much higher than in closely related taxa (e.g., *Batrachotomus kupferzellensis*, Gower and Schoch 2009; *Postosuchus alisonae*, Peyer et al., 2008; *Stagonosuchus nyassicus*, Gebauer 2004).

A mostly complete caudal vertebra (UW ll562-U; Fig. 8E-F) comprises a nearly complete centrum and part of the neural arch. We interpret this as a more anterior caudal vertebra given that the centrum is about as tall as long, lacks any clear facets for the chevron, and the transverse processes, although broken, are large and similar to those of the anterior caudal vertebrae of *Prestosuchus chiniquensis* (SNSB-BSPG AS XXV 3b; Desojo et al. 2020). The anterior articular facet of the centrum (Fig. 8F) is ellipsoidal with a dorsoventral height of five centimeters compared to a mediolateral width of four centimeters. Additionally, the anterior articular facet is shallowly concave like the other vertebrae throughout the column. The centrum is constricted just posterior to the well-defined rim of the anterior articular facet. Only a small fraction of the posterior articular facet is preserved. The anterior portion of the neural arch is intact with the bases of the prezygapophyses. The articular facets of the prezygapophyses are low ~20^{o} to the horizontal. Dorsal to the neural canal, the beginnings of the neural spine project dorsally, flanking a deep interspinous cleft (Fig. 8E) as in *Saurosuchus galilei* (Sill, 1974). As in the other vertebrae described, the neural canal expands ventrally into the dorsal surface of the centrum.

A number of partial centra of distal caudal vertebrae are preserved (UW ll563-A-C; UW 11562-BW); none preserve the neural spine. The posterior caudal vertebrae are typical of archosaurs (e.g., *Postosuchus alisonae*; NCSM 13731) in that the centrum length would be longer than tall, they lack lateral processes, and the middle of the centrum is only slightly

854 constricted relative to the articular ends. The width of the centrum (Fig. 8G-H) is similar to those
855 of *Postosuchus kirkpatricki* (TTUP 9002), but do not appear to be unique among archosaur
856 given the paucity of posterior caudal vertebrae associated with diagnostic material.
857 A number of neural spines were found among the surface collected material, but the
858 exact position of each neural spine within the vertebral column cannot be reconstructed
859 precisely. The height of the neural spines are difficult to estimate, but most of a neural spine
860 (UW ll562-V; Fig. 8E) shows that at least some of the neural spines were about twice the height
861 of a trunk centrum. The neural spines are blade-like in anterior and posterior views and clearly
862 bear lateral expansions at the dorsal end of the spine. The lateral expansions are globular in
863 lateral view and obtain their greatest lateral expansion near the anteroposterior center (UW
864 ll562-CT) or slightly posterior to the anteroposterior center. Additionally, the lateral expansions
865 appear to not expand anteriorly or posterior compared to the rest of the neural spine. There is
866 clear variation in the sample; the lateral expansions are greater in some specimens (UW ll562-
867 CT) compared to others (UW ll562-V). In dorsal view, some appear nearly circular (UW ll562-
868 CX) whereas others are more heart shape with a posterior prong present at the midline (UW
869 ll562-CT). These expansions, referred to spine tables by some authors (e.g., see Nesbitt 2011),
870 commonly occur in non-crocodylomorph loricatans such as *Batrachotomus kupferzellensis*
871 (Gower and Schoch 2009), *Stagonosuchus nyassicus*, (Gebauer 2004), *Saurosuchus galilei*
872 (Trotteyn et al. 2011), *Prestosuchus chiniquensis* (ULBRA-PVT-281; Roberto-Da-Silva et al.
873 2018), and in the cervical vertebrae of *Postosuchus kirkpatricki* (Weinbaum 2013), and clearly
874 outside the group (e.g., *Nundasuchus songeaensis* Nesbitt et al. 2014). The morphology of the
875 lateral expansions of the dorsal portion of the neural spines are abundant enough to support
876 that both the cervical and the trunk vertebrae had the feature, as in *Batrachotomus*
877 *kupferzellensis* (Gower and Schoch 2009).
878

879 **Osteoderm:** A single osteoderm (Fig. 8K-M) was recovered among the holotype in 2010 (TMM
880 unnumbered). The size of the osteoderm is consistent with that of *Heptasuchus clarki*, but it is
881 impossible to conclude that the osteoderm definitely belonged to *Heptasuchus clarki*. The
882 semicircular osteoderm has a nearly flat outer surface covered in small foramina and a few
883 short canals connecting some of the foramina. The ventral surface is nearly smooth with small
884 crisscrossing bone fibers as in most archosauriform osteoderms. In lateral view, the osteoderm
885 is compressed and dorsal and ventral sides are parallel for much of their length, both sides
886 taper toward the edges. The location of the osteoderm on the skeleton is not known and there is
887 no anterior process is present as in most pseudosuchians (Nesbitt 2011).
888
889 **Scapula**: Two partial scapulae, consisting solely of the glenoid region, are known from the
890 accumulation. The larger specimen (UW 11566-B) is from the right side and the smaller
891 specimen (UW11565-E; Fig. 9A) is from the right side. The larger specimen indicates that the
892 coracoid may be partially coossified to the scapula whereas the smaller specimen clearly has a
893 contact surface with the coracoid. The glenoid is well defined by a rim and the glenoid itself is
894 weakly concave. The glenoid opens posteriorly with a lateral component, but the exact angle
895 cannot be determined because the rest of the scapula is not present; the orientation of what is
896 preserved is similar to that of *Batrachotomus kupferzellensis* (SMNS 80271). Just distal to the
897 glenoid on the posterior edge, a rugose scar marks the surface for origin of M. triceps as in
898 other archosaurs (Gower and Schoch, 2009). This scar in is rugose and distinct in *Heptasuchus*
899 *clarki*, but not nearly as laterally expanded compared to that of *Batrachotomus kupferzellensis*
900 (SMNS 80271).
901
902 **Coracoid:** Two fragmentary coracoids (UW 11566; Fig. 9B) were recovered as float during the
903 initial excavation. Both coracoids consist of the more robust glenoid region with a broad
904 articulation surface with the scapula. The laterally concave articulation surface with the humerus

905 (=glenoid) project posterolaterally like that of *Batrachotomus kupferzellensis* (SMNS 80271) and
906 *Postosuchus kirkpatricki* (TTUP 9002). In proximal view, the rugose articulation surface with the
907 scapula is triangular and extends laterally into a small peak. The anterolateral surface just distal
908 to this articulation surface is striated and flat. A clear coracoid foramen is present anterior to the
909 largest articulation surface with the scapula. The foramen is only partially complete in both
910 specimens; but shows that the foramen nearly contacted the scapula articulation surface on the
911 medial surface. The medial surface is flat. It is not clear if the coracoid of *Heptasuchus clarki*
912 had a postglenoid process.
913
914 **Humerus:** A proximal portions of a left humerus (UW 11565-A; Fig. 9C-D) and the proximal
915 portion of a second left humerus (UW ll563-U) are represented among the paratype material of
916 *Heptasuchus clarki*. The latter bone; collected outside the quadrant system is weathered, but
917 clearly indicates the presence of a slightly smaller individual from the locality.
918 The surfaces of UW ll565-A are well preserved. The overall proportions of the humerus
919 cannot be specifically determined because the shaft and distal end are missing. However, it is
920 clear the that proximal expansion relative to the shaft would have been less in *Heptasuchus* and
921 other forms like *Batrachotomus kupferzellensis* (SMNS 80276), *Postosuchus kirkpatricki* (TTUP
922 9002), *Ticinosuchus ferox*, and crocodylomorphs rather than the largely expanded proximal
923 portions of *Stagonosuchus nyassicus* (GPIT/RE/3832), and aetosaurs and their close relatives
924 (e.g., *Parringtonia gracilis*, NMT RB426) where the medial and lateral edges diverge at a greater
925 angle proximally. The proximal surface of the bone is rugose possibly indicating that ossification
926 of the proximal end was not complete at the time of death. The proximal surface lacks a
927 rounded ‘head’ as present in *Batrachotomus kupferzellensis* (SMNS 80276), *Postosuchus*
928 *kirkpatricki* (TTUP 9002), and early crocodylomorphs (Nesbitt, 2011). In proximal view, the
929 medial portion expands relative to the narrower middle to lateral portion. In posterior view, the
930 medial portion of the proximal surface is rounded and is deflected distally. More laterally, the

proximal surface bears a distinct peak near the origin of the deltopectoral crest. The distinct peak (Fig. 9C-D), which is best observed in posterior view, occurs in *Batrachotomus kupferzellensis* (SMNS 80276) and *Stagonosuchus nyassicus* (GPIT/RE/3832), to a lesser extent in *Mandasuchus tanyauchen* (NHMUK PV R6793), but absent in *Postosuchus kirkpatricki* (TTUP 9002) and early crocodylomorphs (Nesbitt, 2011). Broken in UW ll565-A, the deltopectoral crest of UW ll563-U shows that the structure is continuous with the proximal surface, as in *Mandasuchus tanyauchen* (NHMUK PV R6793) and *Batrachotomus kupferzellensis* (SMNS 80276) and not distally shifted as in *Postosuchus kirkpatricki* (TTUP 9002), and early crocodylomorphs (Nesbitt, 2011). The apex of the deltopectoral crest, which is triangular in lateral view, is located in a similar position as in *Batrachotomus kupferzellensis* (SMNS 80276). The anterior surface of the proximal portion is concave whereas the posterior surface is nearly flat. A weakly defined scar is present on the posterolateral side of the posterior surface and is equivalent to a scar in *Batrachotomus kupferzellensis* (SMNS 80276), interpreted to be the surface for origin of M. triceps (Gower and Schoch, 2009).

Ulna: A complete right ulna (UW ll562-W) and a nearly complete left ulna (UW ll562-X) are included as a referred specimen (Fig. 10I-L). Additionally, the distal ends of two other ulnae (UW ll563-V and UW ll565-C) are present indicating that at least three individuals were buried together at the locality. UW ll562-W measures 23.5 cm long and is nearly as long as the complete tibia (UW 11562-Z), but the ulna has a much smaller radius throughout the shaft. The ulna has an expanded proximal portion relative to the shaft and the shaft narrows distally for 2/3rds the length of element and then slightly expands at the distal end (Fig. 10). The expanded proximal end of the ulna bears a moderately developed olecranon process as demonstrated by UW ll562-X (Fig. 10I-L). It appears that the olecranon process of UW ll562-W was a separate ossification and was not fused onto the proximal surface at the time of death. Comparatively, the olecranon is relatively smaller in *Heptasuchus clarki* than that of aetosaurs (e.g.,

957 *Stagonolepis robertsoni*, Walker 1961), *Postosuchus kirkpatricki* (TTUP 9002), *Batrachotomus*
958 *kupferzellensis* (SMNS 80275), and crocodylomorphs (e.g., *Hesperosuchus agilis*, Colbert
959 1952) and is more similar in size to that of *Ticinosuchus ferox* (Krebs 1965) and *Mandasuchus*
960 *tanyauchen* (NHMUK PV R6793. The proximal surface is rugose and triangular (Fig. 10E, I) with
961 a distinct radial tuber but this tuber is not as well expanded as that of *Postosuchus kirkpatricki*
962 (TTUP 9000). The radial tuber extends distally for about 1/3 the length of the ulna. The medial
963 side of the proximal portion is concave as in *Batrachotomus kupferzellensis* (SMNS 80275). The
964 shaft of the ulna is circular, and the anterior surface of the bone bears a longitudinal ridge,
965 which twists medially toward the distal end where a narrow groove is formed between it and the
966 medial edge of the bone. This ridge and groove appear to be presnt in both UW ll562-W and
967 UW ll562-X and is autapomorphic for *Heptasuchus clarki* (see diagnosis). The rugose distal
968 surface is ovoid in outline with a slightly tapered anterolateral end.
969
970 **Radius –** Only the ends of the radius have been identified from weathered fragments, but siding
971 these elements is difficult. The proximal portion is represented by UW 11566-T and UW 11562-
972 DM (Fig. 10AB) and the possible distal ends are represented by UW 11562-DF and UW 11562-
973 DI (Fig. 10CD). The proximal end is mediolaterally compressed with anterior and posterior
974 tapered ends. A concave surface, in lateral view, lies between the anterior and posterior ends of
975 the proximal surface. The distal end is rounded anteriorly and possibly posteriorly also, but this
976 cannot be confirmed because the posterior portion is broken. The distal end of the radius
977 appears similar to that of *Postosuchus alisonae* (NCSM 13731).
978
979 **Ilium:** A fragment consisting of much of the pubic peduncle, and part of the acetabulum is the
980 only positively recognized part of the of the ilium known (UW 11563-Y and UW 11563; Fig.11F).
981 In anteroventral view, the articulation surface with the pubis is rugose and triangular. The
982 acetabular portion that is preserved is concave and the acetabulum appears to be imperforate,

983 as expected for a non-crocodylomorph pseudosuchian. A smooth surface within the acetabulum
984 is present.
985
986 **Pubis:** A nearly complete left pubis (UW ll562-Y; Fig. 11A-D) of *Heptasuchus clarki* was
987 recovered; only parts of the thin medial portion of the pubic apron is not preserved. The pubis is
988 ~37 cm in length from the articulation surface with the ilium to the distal surface. In lateral view,
989 the bone is nearly straight along its entire length like that of *Batrachotomus kupferzellensis*
990 (SMNS 80270). The proximal surface of the pubis, articulates with the pubis peduncle of the
991 ilium) dorsally and ventrally, the proximal portion of the pubis contributes only a minor portion of
992 the edge of the acetabulum as in *Saurosuchus galilei* (Sill, 1971). Distally, the proximal portion
993 narrows in lateral view and transitions into the shaft laterally and medially with the pubic apron.
994 The lateral surface of the proximal portion bears a fossa surrounded by a rugose surface as in
995 *Batrachotomus kupferzellensis* (SMNS 80270); this surface marks the hypothesized site of
996 origin of the *M. ambiens* (Gower and Schoch, 2009). Medially, the proximal portion of the apron
997 is broken so that that the exact size of the obturator fenestra cannot be determined, but it
998 appears to be small more like that of *Batrachotomus kupferzellensis* (Gower and Schoch 2009)
999 than the larger opening in *Postosuchus kirkpatricki* (Weinbaum, 2013). The anteroposterior
1000 thickened medial process marks the proximal articulation with its antimere as in nearly all
1001 paracrocodylomorphs.
1002 In posterior and anterior views, the shaft bows laterally (Fig. 11B) and a similar bowing is
1003 does not appear to be in other paracrocodylomorphs. The shaft is rounded laterally and tapers
1004 to an anteroposteriorly thinner apron medially. The lateral surface of the shaft is smooth without
1005 any ridges.
1006 The distal expands in the last tenth of the length of the pubis. In lateral view, the anterior
1007 end slightly expands at its distalmost margin whereas the posterior edge expands comparatively
1008 more to form an asymmetric expansion (or boot). The distal margin, in lateral view, is rounded.

In anterior view, the pubis shaft medial to the distal expansion is directed posteromedially where it presumably meets its antimere. Consequently, the posteromedial surface of the pubis is distinctly concave (Fig. 11D). The configuration is in contrast to that of *Batrachotomus kupferzellensis* (SMNS 80279), *Arizonasaurus babbitti* (MSM 4590), *Postosuchus alisonae* (NCSM 13731), and *Poposaurus gracilis* (TMM 43683-1) where the apron is orientated directly medially (Nesbitt, 2011). The shape of the distal expansion of *Heptasuchus clarki* is rounded like that of taxa like *Batrachotomus kupferzellensis* (SMNS 80279) and not the mediolaterally narrower expansions of poposauroids (Nesbitt, 2011). The distal surface is rugose.

Ischium: The proximal portion of the right ischium (UW ll564-B; Fig. 11E) was recovered. The proximal portion of the ischium bears a well-defined ridge the demarcates the posteroventral portion of the acetabulum as in *Batrachotomus kupferzellensis* (SMNS 52970). The robust proximal portion has two articulation surfaces at its proximal edge, a dorsal one for articulation with the ilium and a ventral one for articulation with the pubis. The dorsal and ventral articular surfaces are divided in lateral view a portion of the ischium that may have not have articulated with either the ilium or the pubis and, therefore, there may have been a slight gap between the ischium, ilium, and pubis, like that reconstructed for *Batrachotomus kupferzellensis* (Gower and Schoch 2009; Figure 5E). Just posterior to the acetabular rim, a clear pit is present on the dorsal edge. This pit occurs in a variety of archosauromorphs (Ezcurra, 2016) although its length and form differ among archosaurs (Gower and Schoch, 2009).

The shape of the shaft cannot be determined with the preserved portion. The medial surface of the proximal portion of the ischium is flat and the medial and ventral edges indicate that the ischia contacted each other near the proximal portion, similar to other paracrocodylomorphs (e.g., *Postosuchus kirkpatricki*, Weinbaum 2013; *Batrachotomus kupferzellensis*, SMNS 52970; *Arizonasaurus babbitti*, Nesbitt, 2005).

Femur: Two badly worn fragments representing the proximal and distal ends of a right femur (UW ll563-B, UW ll563-A, respectively; Fig. 12A-D) were recovered; it is not clear if both ends belong to the same bone. The proximal surface bears a groove like that of poposauroids and some loricatans (e.g., *Postosuchus kirkpatricki*, Weinbaum, 2013) and all three proximal tubera (sensu Nesbitt, 2005; 2011) appear to be present, although the anteromedial tuber is highly eroded. The preserved portions of the shaft appear to be thin walled like other paracrocodylomorphs (Nesbitt, 2011), but the exact ratio of the thickness of the cortex versus the diameter could not be determined. The distal end bears a small crista tibiofibularis crest and a clear depression is located on the distal surface.

Tibia: The well preserved and complete left tibia of *Heptasuchus clarki* (UW 11562-Z; Fig. 12E-H) is robust with a wide midshaft compared to the length (= 24.0 cm) of the element. The proximal portion does not expand as much relative to the shaft like in *Batrachotomus kupferzellensis* (SMNS 52970). The proximal surface (maximum length = 7 cm) is roughly triangular with a short cnemial crest and rounded lateral surface for articulation with the fibula. The lateral portion of the proximal surface is depressed like that of suchian archosaurs (Nesbitt, 2011) and this surface is separated by the posterior portion of the tibia by a vertical gap (Fig. 12). The proximal surface is highly rugose.

The shaft of the tibia remains oval in section throughout its length, and like the femur, the tibia is also thin walled. The posterior surface of the entire bone, in contrast to the other faces, is flattened, and exhibits a slight twisting along its length. The distal end of the tibia (maximum width = 6 cm) is expanded less than the proximal end and is triangular in distal view. The differentiation of the distal surface of tibia for articulation with the astragalus is poor; the ‘cork-screw’ configuration (proximally slanted posterolateral surface and distally expanded anteromedial portion) typical in shuvosaurids (Nesbitt, 2007), aetosaurs (Parrish 1993), *Batrachotomus kupferzellensis* (SMNS 52970) and in rauisuchids taxa like *Postosuchus*

kirkpatricki (TTUP 9002) is not present in *Heptasuchus clarki*. Instead the distal surface is flatter in *Heptasuchus clarki* and is more like that of *Prestosuchus chiniquensis* (von Huene, 1942; Desojo et al. 2020). The distal surface is also rugose.

Fibula: The fibula is only represented by the right (?) proximal portion (UW 11566-S) and right distal portion (11566-R) recovered among weathered fragments (Fig. 12I-L). The robust proximal portion is asymmetrical in lateral view with a tapering posterior portion. The distal end expands anteriorly and posteriorly and possess an oval distal surface (with an anteroposteriorly long axis).

Metatarsals and phalanges: A number of fragmentary metatarsals (UW 11562-DH, UW 11562-DHU, UW 11562-DR) and phalanges were recovered from the locality and all pes elements consist of weathered proximal or distal ends. Given the difficulty of assigning fragments of metatarsal, we are hesitant to assign anatomical positions to the fragments. However, it is worth noting a few characteristics. The proximal surfaces of the metatarsals have rugose surfaces and are typically rectangular with well-defined faces. The distal end of the metatarsals poses large articular facets that are about as long as wide. A single ungual (UW 11562-DT), possibly from the pes, indicates that the unguals were dorsoventrally flattened like that of *Prestosuchus chiniquensis* (von Huene, 1942).

Phylogenetic Analysis

The phylogenetic position of *Heptasuchus clarki* was assessed using the early archosaur matrix of Nesbitt (2011) as a base followed by the modifications of characters, scores, and terminal taxa of Butler et al. (2014), Nesbitt et al. (2014), Nesbitt and Desojo (2017); Nesbitt et al. (2017), Nesbitt et al. (2018), Butler et al. (2018), and Desojo et al. (2020) and additions of

terminal taxa by Lacerda et al. (2016; 2018) and von Baczko et al. (2014). We added the additional and new characters of Desojo et al. (2020; characters 414 – 422 here), the aphanosaur-centered characters of Nesbitt et al. (2017; characters 434-439 here), a character for rauisuchids and kin from Brusatte et al. (2008; 2010; character 424 here), and nine new characters centered on *Heptasuchus* clarki relationships among loricatans (characters 425-433 here; see appendix 1) for a total of 439 characters. Our primary dataset consists of 100 terminal taxa (supplemental information). This dataset now contains the most specimens and species level terminal taxa of paracrocodylomorphs to date. The matrix includes some stem archosaurs, but for better taxon and character sampling see Ezcurra (2016) and likewise, for better taxon and character sampling for Dinosauria see the dataset of Baron et al. (2017a) and further modifications (e.g., Langer et al. 2017; Baron et al. 2017b).

The matrix was constructed in Mesquite (Madison and Madison 2015) and analyzed with equally weighted parsimony using TNT v. 1.5 (Goloboff and Catalano 2016). Using parsimony, we used new technology search (with the following boxes checked: Sectorial Search, Drift, and Tree Fusing) until 100 hits to the same minimum length. These trees were then run through a traditional search (search trees from RAM option) using TBR branch swapping. *Euparkeria* was set as the outgroup. Zero length branches were collapsed if they lacked support under any of the most parsimonious reconstructions. Characters 32, 52, 121, 137, 139, 156, 168, 188, 223, 247, 258, 269, 271, 291, 297, 314 328, 356, 371, 399 and 413 were ordered - 21 total. We ordered characters 314 and 371 based on the character descriptions of Nesbitt (2011) – characters were not listed in the ordered state list in character sampling and methods.

We ran the first analysis *a priori* excluding the following terminal taxa: *Lewisuchus admixtus*, *Pseudolagosuchus majori* (combined into *Lewisuchus*/*Pseudolagosuchus* following Nesbitt et al. 2010, Nesbitt 2011 and Ezcurra et al. 2019), '*Prestosuchus loricatus* paralectotype' (Desojo et al. 2020), and collapsed *Prestosuchus chiniquensis* lectotype, *Prestosuchus chiniquensis* paralectotype, *Prestosuchus chiniquensis* type series, UFRGS PV 156 T, UFRGS

PV 152 T, CPEZ 239b into a '*Prestosuchus chiniquensis* ALL' (with the addition of scores from ULBRA-PVT-281; Roberto-Da-Silva et al. 2018), added to another description (UFRGS-PV-0629-T; Mastrantonio et al. 2019; see supplemental information). This data matrix resulted in 144 most parsimonious trees (MPTs) of length (1553 steps) (Consistency Index = 0.330; Retention Index = 0.749) (See supplemental information for full tree; S1).

In our main analysis, we also eliminated *Nundasuchus songeaensis* and *Pagosvenator candelariensis* from the final analysis because 1) *Nundasuchus songeaensis* likely is closer to the base of Archosauria (see Nesbitt et al. (2014) and 2) *Pagosvenator candelariensis* is clearly a member Erpetosuchidae (Lacerda et al. 2018), but because of missing information and some character conflict, the taxon is highly unstable (see Desojo et al. 2020). Both taxa could greatly impact the optimizations of character states at the base of and within Paracrocodylomorpha which is the target portion of the Pseudosuchian tree here. This data matrix resulted in 72 most parsimonious trees (MPTs) of length (1529 steps) (Consistency Index = 0.335; Retention Index = 0.752) (Fig. 13 for partial tree; See supplemental information for full tree; S2).

Discussion

The phylogenetic position of *Heptasuchus clarki* among archosaurs:

The results of both our analyses (supplemental information) is similar to the original analysis of Nesbitt (2011) where classic 'Rauisuchia' is a paraphyletic group relative to Crocodylomorpha in 'Rauisuchia' is divided among loricatans (paracrocodylomorph taxa closer to Crocodylomorpha), poposauroids (paracrocodylomorph taxa closer to *Shuvosaurus inexpectatus*), and a few taxa just outside Paracrocodylomorpha (e.g., *Mandasuchus tanyauchen*, *Ticinosuchus ferox*). Unsurprisingly, this pattern has been retained in most iterations of the Nesbitt (2011) dataset (Butler et al. 2011; 2014; 2018; Baczko et al. 2014; Lacerda et al. 2016; 2018; Nesbitt and Desojo 2017; Nesbitt et al. 2014; 2017; 2018; Desojo et al. 2020). Like these other analyses, the base of Paracrocodylomorpha is poorly supported with

the addition or removal of a taxon, a character score change, or the addition of new characters that alter the relationships of these early diverging taxa (e.g., *Mandasuchus tanyauchen*, *Stagonosuchus nyassicus*). Within Loricata, *Saurosuchus galilei*, *Prestosuchus chiniquensis*, and *Luperosuchus fractus* consistently are located at the base of the clade. The relationship of these taxa could be a grade (as found here) or in a clade (Nesbitt and Desojo 2017; Desojo et al. 2020) as a consequence of character optimizations for taxa closer to Crocodylomorpha. Moreover, we did not find *Stagonosuchus* (=*Prestosuchus* Desojo et al. 2020) *nyassicus* as the sister taxon of *Prestosuchus chiniquensis* with the addition of our new characters (see appendix), but given that the new characters focus on the skull and *Stagonosuchus nyassicus* is almost only represented by postcrania, this instability is not surprising. The relationship within loricatans closer to Crocodylomorpha (i.e., *Batrachotomus kupferzellensis* + *Alligator mississippiensis*) remained unchanged in comparison with Nesbitt (2011).

Heptasuchus clarki is well nested within Loricata and firmly supported as the sister taxon of *Batrachotomus kupferzellensis.* The following unambiguous character states support this relationship: dorsal (=ascending) process of the maxilla remains the same width for its length (29-0) (? in *Heptasuchus clarki*); posterior portion of the nasal are concave at the midline in dorsal view (34-1); anterior portion of the frontal tapers anteriorly along the mid-line (43-1) (? in *Heptasuchus clarki*); squamosal with distinct ridge on dorsal surface along edge of supratemporal fossa (49-1) (? in *Heptasuchus clarki*); double-headed ectopterygoid (89-1) (? in *Heptasuchus clarki*); supratemporal fossa present anterior to the supratemporal fenestra (144-1).

Heptasuchus clarki is well supported as the sister taxon of *Batrachotomus kupferzellensis*. The following unambiguous character states support this relationship: anterodorsal margin at the base of the dorsal process of the maxilla concave (25-1); dorsolateral margin of the anterior portion of the nasal with a distinct anteroposteriorly ridge on the lateral edge (35-1); depression on the anterolateral surface of the ventral end of the

postorbital (425-1); distinct fossa on the posterodorsal portion of the naris on the lateral side of the nasal (430-1); anteroposteriorly trending ridge on the lateral side of the jugal is asymmetrical dorsoventrally where the dorsal portion is more laterally expanded (433-1). The crania of *Heptasuchus clarki* shares a number of unique features with *Batrachotomus kupferzellensis*, many of which were once considered autapomorphies of *Batrachotomus kupferzellensis* (Gower 1999). However, we were not able to pinpoint any postcranial character states that *Batrachotomus kupferzellensis* and *Heptasuchus clarki* share exclusively.

***Heptasuchus clarki* and *Poposaurus gracilis*:**

When initially described, *Heptasuchus clarki* was considered to be from the Popo Agie Formation which also contained the remains of another 'rauisuchian' *Poposaurus gracilis*. Long and Murry (1995) hypothesized that *Heptasuchus clarki* may be a poposauroid after comparisons with *Poposaurus gracilis*, *Shuvosaurus* (= 'Chatterjeea') *elegans* and *Postosuchus kirkpatricki*. Soon after, Zawiskie and Dawley (2003) hypothesized that the skull of *Heptasuchus clarki* might belong to the body of *Poposaurus gracilis* based on age proximity and on a few overlapping postcranial bones. After further analyses, we now reject these hypotheses based on a number of lines of evidence. First of all, our robust phylogenetic analysis clearly places *Heptasuchus clarki* and *Batrachotomus kupferzellensis* as close relatives and both are more closely related to crocodylomorphs than poposauroids. Second, the deposits that *Heptasuchus clarki* was found in are likely not the same as the Popo Agie Formation from the western portion of Wyoming and the deposits that *Heptasuchus clarki* was found in are likely older than that of the Popo Agie Formation and hence *Poposaurus gracilis*. Third, with an abundance of new specimens of *Poposaurus gracilis* from partial skeletons (Weinbaum and Hungerbühler 2007) to nearly complete and articulated postcranial remains (Gauthier et al. 2011; Schachner et al. 2019), and comparative skull material (Parker and Nesbitt 2013), it is clear the *Poposaurus gracilis* and *Heptasuchus clarki* are different taxa.

Further implication from *Heptasuchus clarki*:

The stratigraphic and temporal occurrence of *Heptasuchus clarki* fills a critical gap in loricatan biogeography within current-day North America and across Pangea. *Heptasuchus clarki* is the only confirmed loricatan taxon from either the late Middle Triassic or the early portion of the Late Triassic (see above) and demonstrates that large paracrocodylomorphs were present from the early portion of the Middle Triassic (i.e., *Arizonasaurus babbitti* and other forms from the Moenkopi Formation; Nesbitt 2003; Schoch et al. 2010) through the end of the deposition of Upper Triassic strata (*Effigia okeeffeae* 'siltstone member,' *Coelophysis* Quarry). Furthermore, *Heptasuchus clarki* fills a 'phylogenetic gap' in that it is the only named loricatan from current-day North America that does not fit into Poposauroidea (Ctenosauriscidae or Shuvosauridae) or Rauisuchidae (e.g. *Postosuchus*, *Viviron haydeni*) and links these disparate clades present in current-day North America to forms from current-day South America and Europe. The presence of a 'mid-grade' loricatan in current-day North America hints that earlier diverging loricatans known from current-day South America (*Prestosuchus chiniquensis*, *Luperosuchus fractus*, *Saurosuchus galilei*) may have had close relatives in current-day North America, but equivalently-aged deposits in North America are lacking.

The sister taxon relationship of *Heptasuchus clarki* and *Batrachotomus kupferzellensis* demonstrates the first biotic link between current-day North America in the Middle to early Late Triassic and the Middle Triassic (Ladinian Stage) of current-day Germany. Although the assemblage from the *Heptasuchus clarki* bonebed has not been studied in detail (see above), there are no other overlapping species or genus-level taxa that are present from the *Heptasuchus clarki* bonebed and the *Batrachotomus kupferzellensis* locality (= Kupferzell = Lagerstätte Kupferzell-Bauersbach), let alone major clades (e.g., the temnospondyls *Gerrothorax*, *Plagiosuchus*, *Mastodontosaurus*, *Kupferzellia*, *Trematolestes*, the chronosuchian *Bystrowiella schumanni*, Choristodera, the sauropterygian *Nothosaurus*; Hagdorn et al. 2015

and a variety of smaller tetrapods represented by jaw material or tooth distinct morphologies; Schoch et al. 2018). Moreover, the clades present in the Ladinian-aged Kupferzell locality of current-day Germany are either completely absent or rare in North America during the entire Triassic Period (e.g., the temnospondyls, chronosuchian). The similarity of just the large carnivorous archosaurs between current day North America and Germany in highly differentiated vertebrate assemblages implies that the larger archosaurs may have had significant flexibility in their paleoenvironments across Pangea through the Middle to Upper Triassic. This notion is further supported by the evidence presented by Nesbitt et al. (2009) suggesting that carnivorous archosaurs (e.g., dinosaurs and crocodylomorphs) may have had greater distribution in the environments across Pangea.

The holotype locality of *Heptasuchus clarki* contains a minimum of four individuals and this occurrence appears to be common with paracrocodylomorphs archosaurs, at least in the Triassic Period. The exact number of individuals is not known because of the heavily weather bonebed, but it is clear that some individuals were highly scattered and disarticulated whereas some other individuals, including the holotype, were closely associated. The closest relative of *Heptasuchus clarki, Batrachotomus kupferzellensis* was also found in a similar condition: associated and disarticulated individuals across a bonebed (i.e., Lagerstätte Kupferzell-Bauersbach; Gower 1999). Finding non-crocodylomorph paracrocodoylomorphs (or ‘rauisuchians’) in bonebeds with more than one individual appears common across the clade from the Middle to Upper Triassic across Pangea. For example, multiple individuals of *Heptasuchus clarki, Batrachotomus kupferzellensis*, *Postosuchus kirkpatricki*, *Effigia okeeffeae*, *Shuvosaurus inexpectatus*, and *Decuriasuchus quartacolonia* have been found together in the same deposits. The preservation of these paracrocodylomorphs ranges from nearly complete skeletons to disarticulated, but associated skeletons. The implications of the association of these individuals to behavior must be carefully considered on a variety of anatomical, taphonomic and sedimentalogical data (França et al. 2011), but the repeated co-occurrence of

individuals of paracrocodylomorphs is intriguing and may suggest that these reptiles were typically in groups (França et al. 2011) and this behavior was maintained through much of their evolutionary history.

Institutional Abbreviations

ALM, refers to 'Alili n'yifis' locality near the village of Alma. Specimens stored at Museum National d'Histoire Naturelle, Paris, France (MNHN); **BPI**, Evolutionary Studies Institute (formerly Bernard Price Institute for Palaeontological Research), University of the Witwatersrand, Johannesburg, South Africa; **CPEZ**, Coleção de Paleontologia do Museu Paleontológico Arqueológico Walter Ilha, São Pedro do Sul, Brazil; **GPIT**, Institut und Museum für Geologie und Paläontologie, Universität Tübingen, Germany; **IVPP**, Institute of Vertebrate Paleontology and Paleoanthropology, Beijing, China; **MSM**, Arizona Museum of Natural History, Mesa, Arizona, USA; **NCSM**, North Carolina Museum of Natural Sciences, Raleigh, North Carolina, USA; **NHMUK** (formerly BMNH), Natural History Museum, London, U.K.; **NMMNH**, New Mexico Museum of Natural History and Science, Albuquerque, New Mexico, USA; **NMT**, National Museum of Tanzania, Dar es Salaam, Tanzania; **PEFO**, Petrified Forest National Park, Arizona, USA; **PULR**, Paleontología, Universidad Nacional de La Rioja, La Rioja, Argentina; **PVL**, Paleontología de Vertebrados, Instituto "Miguel Lillo", San Miguel de Tucumán, Argentina; **PVSJ**, División de Paleontología de Vertebrados del Museo de Ciencias Naturales y Universidad Nacional de San Juan, San Juan, Argentina; **SAM**, Iziko South African Museum, Cape Town, South Africa; **SMNS**, Staatliches Museum für Naturkunde, Stuttgart, Germany; **SNSB-BSPG**, Staatliche Naturwissenschaftliche Sammlungen Bayerns, Bayerische Staatssammlung für Paläontologie und Geologie, Munich, Germany; **TMM**, Texas Vertebrate Paleontology Collections, The University of Texas at Austin, Texas, USA; **TTU**, Texas Tech University Museum, Lubbock, Texas, USA; **UFRGS-PV**, Laboratório de Paleovertebrados,

Universidade Federal do Rio Grande do Sul, Porto Alegre, Brazil; **ULBRA-PVT**, Paleovertebrate Collection of the Universidade Luterana do Brasil, Canoas, Rio Grande do Sul, Brazil; **USNM**, National Museum of Natural History (formerly United States National Museum), Smithsonian Institution, Washington, DC, USA; **UW**, University of Wyoming, Laramie, Wyoming, USA; **ZPAL**, Institute of Paleobiology, Polish Academy of Sciences, Warsaw, Poland.

Acknowledgements

We especially thank Michelle Stocker for conversations about Wyoming geology, Triassic rocks of the western US, and Triassic assemblages. We thank the many insightful conversations about 'rauisuchian' relationships and anatomy with David J. Gower and Julia B. Desojo. The TMM *Heptasuchus clarki* material was collected under a Bureau of Land Management permit facilitated by Dale Hansen. Laura A. Vietti helped located and curate *Heptasuchus clarki* material from the UW collection and J. Chris Sagebiel curated the TMM *Heptasuchus clarki* material.

References

Alcober, O. 2000. Redescription of the skull of *Saurosuchus galilei* (Archosauria: Rauisuchidae). Journal of Vertebrate Paleontology 20:302-316.

Baron, M. G., D. B. Norman, and P. M. Barrett. 2017a. A novel hypothesis of dinosaur relationships and early dinosaur evolution. Nature 543:501–506.

Baron, M. G., D. B. Norman, and P. M. Barrett. 2017b. Baron et al. reply. Nature 551:E4-E5.

Benton, M. J. 1986. The Late Triassic reptile *Teratosaurus* - A rauisuchian, not a dinosaur. Palaeontology 29:293-301.

1290 Benton, M. J., and J. M. Clark. 1988. Archosaur phylogeny and the relationships of the
1291 Crocodylia; pp. 295-338 in M. J. Benton (ed.), The Phylogeny and Classification of the
1292 Tetrapods. Vol 1: Amphibians and Reptiles. Clarendon Press, Oxford.
1293 Bailleul, A. M., J. B. Scannella, J. R. Horner, and D. C. Evans. 2016. Fusion patterns in the
1294 skulls of modern archosaurs reveal that sutures are ambiguous maturity indicators for
1295 the Dinosauria. PLoS One 11: e0147687.
1296 Bittencourt, J. S., A. B. Arcucci, C. A. Marsicano, and M. C. Langer. 2015. Osteology of the
1297 Middle Triassic archosaur *Lewisuchus admixtus* Romer (Chañares Formation,
1298 Argentina), its inclusivity, and relationships amongst early dinosauromorphs. Journal of
1299 Systematic Palaeontology 13:189-219.
1300 Bonaparte, J. F. 1984. Locomotion in rauisuchid thecodonts. Journal of Vertebrate Paleontology
1301 3:210-218.
1302 Brochu, C. A. 1996. Closure of neurocentral sutures during crocodilian ontogeny: implications
1303 for maturity assessment in fossil archosaurs. Journal of Vertebrate Paleontology 16:49-
1304 62.
1305 Brusatte, S. L., M. J. Benton, J. B. Desojo, and M. C. Langer. 2010. The higher-level phylogeny
1306 of Archosauria (Tetrapoda: Diapsida). Journal of Systematic Palaeontology 8:3-47.
1307 Brusatte, S. L., M. J. Benton, M. Ruta, and F. T. Lloyd. 2008. Superiority, competition, and
1308 opportunism in the evolutionary radiation of dinosaurs. Science 321:1485-1488.
1309 Brusatte, S. L., R. J. Butler, T. Sulej, and G. Niedzwiedzki. 2009. The taxonomy and anatomy of
1310 rauisuchian archosaurs from the Late Triassic of Germany and Poland. Acta
1311 Palaeontologica Polonica 54:221-230.
1312 Butler, R. J., S. L. Brusatte, M. Reich, S. J. Nesbitt, R. R. Schoch, and J. J. Hornung. 2011. The
1313 sail-backed reptile ctenosauriscus from the latest Early Triassic of Germany and the
1314 timing and biogeography of the early archosaur radiation. PLoS One 6:1-28.

1315 Butler, R. B., C. Sullivan, M. D. Ezcurra, J. Liu, A. Lecuona, and R. B. Sookias. 2014. New clade
1316 of enigmatic early archosaurs yields insights into early pseudosuchian phylogeny and
1317 the biogeography of the archosaur radiation. BMC Evolutionary Biology 14:1-16.
1318 Butler, R. J., S. L. Brusatte, M. Reich, S. J. Nesbitt, R. R. Schoch, and J. J. Hornung. 2011. The
1319 sail-backed reptile ctenosauriscus from the latest Early Triassic of Germany and the
1320 timing and biogeography of the early archosaur radiation. PLoS One 6:1-28.
1321 Butler, R. J., S. J. Nesbitt, A. J. Charig, D. J. Gower, and P. M. Barrett. 2018. *Mandasuchus*
1322 *tanyauchen* gen. et sp. nov., a pseudosuchian archosaur from the Manda Beds of
1323 Tanzania; pp. 96–121 in C. A. Sidor, and S. J. Nesbitt (eds.), Vertebrate and climatic
1324 evolution in the Triassic rift basins of Tanzania and Zambia. Society of Vertebrate
1325 Paleontology Memoir 17, Journal of Vertebrate Paleontology 37 (6, supplement).
1326 Cavaroc, V. V., and R. M. Flores. 1991. Red beds of the Triassic Chugwater Group,
1327 Southwestern Powder River Basin, Wyoming. US. Geological Survey Bulletin 1917-E,
1328 17.
1329 Chatterjee, S. 1985. *Postosuchus*, a new thecodontian reptile from the Triassic of Texas and the
1330 origin of tyrannosaurs. Philosophical Transactions of the Royal Society of London B
1331 309:395-460.
1332 Clark, J. M., and H.-D. Sues. 2002. Two new basal crocodylomorph archosaurs from the Lower
1333 Jurassic and the monophyly of the Sphenosuchia. Zoological Journal of the Linnean
1334 Society 136:77-95.
1335 Colbert, E. H. 1952. A pseudosuchian reptile from Arizona. Bulletin of the American Museum of
1336 Natural History 99:561-592.
1337 Colbert, E. H. 1989. The Triassic dinosaur *Coelophysis*. Bulletin of the Museum of Northern
1338 Arizona 57:1-174.
1339 Cope, E. D. 1869. Synopsis of the extinct Batrachia, Reptilia, and Aves of North America.
1340 Transactions of the American Philosophical Society 40:1-252.

1341 Dawley, R. M., J. M. Zawiske, and J. W. Cosgriff. 1979. A rauisuchid thecodont from the Upper
1342 Triassic Popo Agie Formation of Wyoming. Journal of Paleontology 53:1428-1431.
1343 de França, M. A. G., J. Ferigolo, and M. C. Langer. 2011. Associated skeletons of a new Middle
1344 Triassic “Rauisuchia” from Brazil. Naturwissenschaften 98:389-395.
1345 de França, M. A. G., M. C. Langer, and J. Ferigolo. 2013. The skull anatomy of *Decuriasuchus*
1346 *quartacolonia* (Pseudosuchia: Suchia: Loricata) from the middle Triassic of Brazil; pp.
1347 469-501 in S. J. Nesbitt, J. B. Desojo, and R. B. Irmis (eds.), Anatomy, Phylogeny and
1348 Palaeobiology of Early Archosaurs and their Kin. Geological Society, London, Special
1349 Publications, London.
1350 Desojo, J. B., M. B. Von Baczko, and O. W. M. Rauhut. 2020. Anatomy, taxonomy and
1351 phylogenetic relationships of *Prestosuchus chiniquensis* (Archosauria: Pseudosuchia)
1352 from the original collection of von Huene, Middle-Late Triassic of southern Brazil.
1353 Palaeontologia Electronica 23:a04. https://doi.org/10.26879/1026palaeo-
1354 electronica.org/content/2020/2917-type-materials-of-prestosuchus.
1355 Ewer, R. F. 1965. The anatomy of the thecodont reptile *Euparkeria capensis* Broom.
1356 Philosophical Transactions of the Royal Society of London, Series B 248:379-435.
1357 Ezcurra, M. D. 2016. The phylogenetic relationships of basal archosauromorphs, with an
1358 emphasis on the systematics of proterosuchian archosauriforms. PeerJ:4:e1778.
1359 Ezcurra, M. D., S. J. Nesbitt, L. E. Fiorelli, and J. B. Desojo. 2019. New specimen sheds light on
1360 the anatomy and taxonomy of the early Late Triassic dinosauriforms from the Chañares
1361 Formation, NW Argentina. Anatomical Record: DOI: 10.1002/ar.24243.
1362 Gauthier, J. A. 1986. Saurischian monophyly and the origin of birds. Memoirs of the California
1363 Academy of Science 8:1-55.
1364 Gauthier, J. A., S. J. Nesbitt, E. Schachner, G. S. Bever, and W. G. Joyce. 2011. The bipedal
1365 stem crocodilian *Poposaurus gracilis*: inferring function in fossils and innovation in
1366 archosaur locomotion. Bulletin of the Peabody Museum of Natural History 52:107-126.

1367 Gebauer, E. V. I. 2004. Neubeschreibung von *Stagonosuchus nyassicus* v. Huene, 1938
1368 (Thecodontia, Rauisuchia) from the Manda Formation (Middle Triassic) of southwest
1369 Tanzania. Neues Jahrbuch für Geologie und Paläeontologie, Abhandlungen 231:1-35.
1370 Goloboff, P. A., and S. A. Catalano. 2016. TNT version 1.5, including a full implementation of
1371 phylogenetic morphometrics. Cladistics 32:221-238.
1372 Gower, D. J. 2000. Rauisuchian archosaurs (Reptilia, Diapsida): An overview. Neues Jahrbuch
1373 für Geologie und Paläontologie Abhandlungen 218:447-488.
1374 Gower, D. J. 2002. Braincase evolution in suchian archosaurs (Reptilia: Diapsida): Evidence
1375 from the rauisuchian *Batrachotomus kupferzellensis*. Zoological Journal of the Linnean
1376 Society 136:49-76.
1377 Gower, D. J., and S. J. Nesbitt. 2006. The braincase of *Arizonasaurus babbitti*- further evidence
1378 of the non-monophyly of Rauisuchia. Journal of Vertebrate Paleontology 26:79-87.
1379 Gower, D. J., and R. Schoch. 2009. Postcranial anatomy of the rauisuchian archosaur
1380 *Batrachotomus kupferzellensis*. Journal of Vertebrate Paleontology 29:103-122.
1381 Gower, D. J., and A. G. Sennikov. 1996. Braincase morphology in early archosaurian reptiles.
1382 Palaeontology 39:883-906.
1383 Gower, D. J., and A. D. Walker. 2002. New data on the braincase of the aetosaurian archosaur
1384 (Reptilia: Diapsida) *Stagonolepis robertsoni* Agassiz. Zoological Journal of the Linnean
1385 Society 136:7-23.
1386 Hagdorn, H., R. Schoch, D. Seegis, and R. Werneburg. 2015. Wirbeltierlagerstätten im
1387 Lettenkeuper; pp. 325–358 in H. Hagdorn, R. R. Schoch, and G. Schweigert (eds.), Der
1388 Lettenkeuper – Ein Fenster in die Zeit vor den Dinosauriern. Staatliches Museum für
1389 Naturkunde Stuttgart, Stuttgart.
1390 High Jr, L. R., and M. D. Picard. 1969. Stratigraphic relations within upper Chugwater group
1391 (Triassic), Wyoming. American Association of Petroleum Geologists Bulletin
1392 53:1091-1104.

1393 Huene, F. v. 1942. Die fossilen Reptilien des Südamerikanischen Gondwanalandes.
1394 Ergebnisse der Sauriergrabungen in Südbrasilien 1928/29. 332 pp. C.H. Beck,
1395 München, Germany.
1396 Irmen, A., and C. Vondra. 2000. Aeolian sediments in Lower to Middle (?) Triassic rocks of
1397 central Wyoming. Sedimentary Geology 132:69-88.
1398 Irmis, R. B. 2007. Axial skeleton ontogeny in the parasuchia (Archosauria: Pseudosuchia) and
1399 its implications for ontogenetic determination in archosaurs. Journal of Vertebrate
1400 Paleontology 27:350-361.
1401 Jalil, N.-E., and K. Peyer. 2007. A new rauisuchian (Archosauria, Suchia) from the Upper
1402 Triassic of the Argana Basin, Morocco. Palaeontology 50:417-430.
1403 Johnson, E. A. 1993. Depositional History of Triassic Rocks in the Area of the Powder River
1404 Basin, Northeastern Wyoming, and Southeastern Montana. US Government Printing
1405 Office.
1406 Juul, L. 1994. The phylogeny of basal archosaurs. Palaeontologia Africana 31:1-38.
1407 Krebs, B. 1976. Pseudosuchia; pp. 40-98 in O. Kuhn (ed.), Handbuch Palaoherpetology. Gustav
1408 Fischer Verlag, Stuttgart.
1409 Lacerda, M. B., M. A. de França, and C. L. Schultz. 2018. A new erpetosuchid (Pseudosuchia,
1410 Archosauria) from the Middle–late Triassic of Southern Brazil. Zoological Journal of the
1411 Linnean Society 184:804-824.
1412 Lacerda, M. B., B. M. Mastrantonio, D. C. Fortier, and C. L. Schultz. 2016. New insights on
1413 *Prestosuchus chiniquensis* Huene, 1942 (Pseudosuchia, Loricata) based on new
1414 specimens from the “Tree Sanga” Outcrop, Chiniquá Region, Rio Grande do Sul, Brazil.
1415 PeerJ 4:e1622.
1416 Langer, M. C., M. D. Ezcurra, O. W. Rauhut, M. J. Benton, F. Knoll, B. W. McPhee, F. E. Novas,
1417 D. Pol, and S. L. Brusatte. 2017. Untangling the dinosaur family tree. Nature 551:E1-E3.

1418 Lautenschlager, S., and J. B. Desojo. 2011. Reassessment of the Middle Triassic rauisuchian
1419 archosaurs *Ticinosuchus ferox* and *Stagonosuchus nyassicus*. Paläontologische
1420 Zeitschrift 85:357-381.
1421 Lautenschlager, S., and O. W. M. Rauhut. 2015. Osteology of *Rauisuchus tiradentes* from the
1422 Late Triassic (Carnian) Santa Maria Formation of Brazil, and its implications for
1423 rauisuchid anatomy and phylogeny. Zoological Journal of the Linnean Society 173:55-
1424 91.
1425 Lessner, E. J., M. R. Stocker, N. D. Smith, A. H. Turner, R. B. Irmis, and S. J. Nesbitt. 2016. A
1426 new taxon of rauisuchid (Archosauria, Pseudosuchia) from the Upper Triassic of New
1427 Mexico increases the diversity and temporal range of the clade. PeerJ 4:e2336.
1428 Long, R. A., and P. A. Murry. 1995. Late Triassic (Carnian and Norian) tetrapods from the
1429 southwestern United States New Mexico Museum of Natural History and Science
1430 Bulletin 4:1-254.
1431 Lovelace, D. M., and A. C. Doebbert. 2015. A new age constraint for the Early Triassic Alcova
1432 Limestone (Chugwater Group), Wyoming. Palaeogeography, Palaeoclimatology,
1433 Palaeoecology 424:1-5.
1434 Lucas, S. G. 1998. Global Triassic tetrapod biostratigraphy and biochronology.
1435 Palaeogeography, Palaeoclimatology, Palaeoeocology 143:347-384.
1436 Lucas, S. G., A. B. Heckert, and N. Hotton III. 2002. The rhynchosaur *Hyperodapedon* from the
1437 Upper Triassic of Wyoming and its global biochronological significance. Bulletin of the
1438 New Mexico Museum of Natural History and Science 21:149-156.
1439 Lucas, S. G., A. B. Heckert, and L. Rinehart. 2007. A giant skull, ontogenetic variation and
1440 taxonomic validity of the Late Triassic phytosaur *Parasuchus*. Bulletin of the New Mexico
1441 Museum of Natural History and Science 41:222-227.
1442 Maddison, W. P., and D. R. Maddison. 2015. Mesquite: a modular system
1443 for evolutionary analysis (version 3.02). Available at http://mesquiteproject.org

1444 Mastrantonio, B. M., M. B. Von Baczko, J. B. Desojo, and C. L. Schultz. 2019. The skull
1445 anatomy and cranial endocast of the pseudosuchid archosaur *Prestosuchus*
1446 *chiniquensis* from the Triassic of Brazil. Acta Palaeontologica Polonica 64:171-198.
1447 Nesbitt, S. J. 2003. *Arizonasaurus* and its implications for archosaur divergences. Proceedings
1448 of the Royal Society of London, B 270(Supplement 2):S234-S237.
1449 Nesbitt, S. J. 2005. The osteology of the Middle Triassic pseudosuchian archosaur
1450 *Arizonasaurus babbitti*. Historical Biology 17:19-47.
1451 Nesbitt, S. J. 2007. The anatomy of *Effigia okeeffeae* (Archosauria, Suchia), theropod
1452 convergence, and the distribution of related taxa. Bulletin of the American Museum of
1453 Natural History 302:1-84.
1454 Nesbitt, S. J. 2011. The early evolution of Archosauria: relationships and the origin of major
1455 clades. Bulletin of the American Museum of Natural History 352:1-292.
1456 Nesbitt, S. J., S. L. Brusatte, J. B. Desojo, A. Liparini, D. J. Gower, M. A. G. d. França, and J. C.
1457 Weinbaum. 2013a. “Rauisuchia”; pp. 241-274 in S. J. Nesbitt, J. B. Desojo, and R. B.
1458 Irmis (eds.), Anatomy, Phylogeny, and Palaeobiology of Early Archosaurs and their Kin.
1459 Geological Society, London, Special Volume.
1460 Nesbitt, S. J., R. J. Butler, M. D. Ezcurra, P. M. Barrett, M. R. Stocker, K. D. Angielczyk, R. M.
1461 H. Smith, C. A. Sidor, G. Niedźwiedzki, A. Sennikov, and A. J. Charig. 2017. The earliest
1462 bird-line archosaurs and assembly of the dinosaur body plan. Nature 544:484-487.
1463 Nesbitt, S. J., R. J. Butler, M. D. Ezcurra, A. J. Charig, and P. M. Barrett. 2018. The anatomy of
1464 *Teleocrater rhadinus*, an early avemetatarsalian from the lower portion of the Lifua
1465 Member of the Manda Beds (~Middle Triassic); pp. 142-177 in C. A. Sidor, and S. J.
1466 Nesbitt (eds.), Vertebrate and climatic evolution in the Triassic rift basins of Tanzania
1467 and Zambia. Society of Vertebrate Paleontology Memoir 17, Journal of Vertebrate
1468 Paleontology 37 (6, supplement).

1469 Nesbitt, S. J., and J. B. Desojo. 2017. The osteology and phylogenetic position of *Luperosuchus*
1470 *fractus* (Archosauria: Loricata) from the latest Middle Triassic or earliest Late Triassic of
1471 Argentina. Ameghiniana 54:261–282.
1472 Nesbitt, S. J., J. Liu, and C. Li. 2011. A sail-backed suchian from the Heshanggou Formation
1473 (Early Triassic: Olenekian) of China. Earth and Environmental Science Transactions of
1474 the Royal Society of Edinburgh 101:271-284.
1475 Nesbitt, S. J., C. A. Sidor, K. D. Angielczyk, R. M. H. Smith, and L. A. Tsuji. 2014. A new
1476 archosaur from the Manda beds (Anisian: Middle Triassic) of southern Tanzania and its
1477 implications for character optimizations at Archosauria and Pseudosuchia. Journal of
1478 Vertebrate Paleontology 34:1357-1382.
1479 Nesbitt, S. J., C. A. Sidor, R. B. Irmis, K. D. Angielczyk, R. M. H. Smith, and L. A. Tsuji. 2010.
1480 Ecologically distinct dinosaurian sister-group shows early diversification of Ornithodira.
1481 Nature 464:95-98.
1482 Nesbitt, S. J., N. D. Smith, R. B. Irmis, A. H. Turner, A. Downs, and M. A. Norell. 2009. A
1483 complete skeleton of a Late Triassic saurischian and the early evolution of dinosaurs.
1484 Science 326:1530-1533.
1485 Nesbitt, S. J., A. H. Turner, and J. C. Weinbaum. 2013b. A survey of skeletal elements in the
1486 orbit of Pseudosuchia and the origin of the crocodylian palpebral. Earth and
1487 Environmental Science Transactions of the Royal Society of Edinburgh 103:365-381.
1488 Parker, W. G., and S. J. Nesbitt. 2013. Cranial remains of *Poposaurus gracilis* (Pseudosuchia:
1489 Poposauroidea) from the Upper Triassic, the distribution of the taxon and its implications
1490 for poposauroid evolution; pp. 503-523 in S. J. Nesbitt, J. B. Desojo, and R. B. Irmis
1491 (eds.), Anatomy, Phylogeny, and Palaeobiology of Early Archosaurs and their Kin.
1492 Geological Society, London, Special Volume.
1493 Parrish, J. M. 1993. Phylogeny of the Crocodylotarsi, with reference to archosaurian and
1494 crurotarsan monophyly. Journal of Vertebrate Paleontology 13:287-308.

1495 Peyer, K., J. G. Carter, H.-D. Sues, S. E. Novak, and P. E. Olsen. 2008. A new suchian
1496 archosaur from the Upper Triassic of North Carolina. Journal of Vertebrate Paleontology
1497 28:363-381.
1498 Picard, M. D. 1978. Stratigraphy of Triassic rocks in west-central Wyoming. Wyoming
1499 Geological Association Resources of the Wind River Basin; 30th Annual Field
1500 Conference Guidebook: 101-130.
1501 Roberto-Da-Silva, L., R. T. Müller, M. A. G. d. França, S. F. Cabreira, and S. Dias-Da-Silva.
1502 2018. An impressive skeleton of the giant top predator *Prestosuchus chiniquensis*
1503 (Pseudosuchia: Loricata) from the Triassic of Southern Brazil, with phylogenetic
1504 remarks. Historical Biology:1-20.
1505 Romer, A. S. 1971. The Chañares (Argentina) Triassic reptile fauna. VIII. A fragmentary skull of
1506 a large thecodont, *Luperosuchus fractus*. Breviora 373:1-8.
1507 Schachner, E. R., R. B. Irmis, A. K. Huttenlocker, S. J. Nesbitt, R. K. Sanders, and R. L. Cieri.
1508 2019. Osteology of the Late Triassic bipedal archosaur *Poposaurus gracilis*
1509 (Archosauria: Pseudosuchia). Anatomical Record:DOI: 10.1002/ar.24298.
1510 Schoch, R. R., and J. B. Desojo. 2016. Cranial anatomy of the aetosaur *Paratypothorax*
1511 *andressorum* Long & Ballew, 1985, from the Upper Triassic of Germany and its bearing
1512 on aetosaur phylogeny. Neues Jahrbuch für Geologie und Paläontologie-Abhandlungen
1513 279:73-95.
1514 Schoch, R., S. J. Nesbitt, J. Muller, M. Fastnacht, S. G. Lucas, and J. A. Boy. 2010. The reptile
1515 assemblage from the Moenkopi Formation (Middle Triassic) of New Mexico. Neues
1516 Jahrbuch für Geologie und Paläontologie, Abhandlungen 255:245-369.
1517 Schoch, R. R., F. Ullmann, B. Rozynek, R. Ziegler, D. Seegis, and H.-D. Sues. 2018. Tetrapod
1518 diversity and palaeoecology in the German Middle Triassic (Lower Keuper) documented
1519 by tooth morphotypes. Palaeobiodiversity and Palaeoenvironments 98:615-638.

1520 Sereno, P. C., S. McAllister, and S. L. Brusatte. 2005. TaxonSearch: a relational database for
1521 suprageneric taxa and phylogenetic definitions. PhyloInformatics 8:1-21.
1522 Sill, W. D. 1974. The anatomy of *Saurosuchus galilei* and the relationships of the rauisuchid
1523 thecodonts. Bulletin of the Museum of Comparative Zoology 146:317-362.
1524 Stocker, M. R. 2010. Clarification of the skeletal anatomy of phytosaurs based on comparative
1525 anatomy and the most complete specimen of *Angistorhinus*. Journal of Vertebrate
1526 Paleontology, Program and Abstracts 2010:170A.
1527 Stocker, M. R., and R. J. Butler. 2013. Phytosauria; pp. 91-117 in S. J. Nesbitt, J. B. Desojo,
1528 and R. B. Irmis (eds.), Anatomy, Phylogeny and Palaeobiology of Early Archosaurs and
1529 their Kin. The Geological Society of London, London.
1530 Sulej, T. 2005. A new rauisuchian reptile (Diapsida: Archosauria) from the Late Triassic of
1531 Poland. Journal of Vertebrate Paleontology 25:78-86.
1532 Trotteyn, M. J., J. B. Desojo, and O. Alcober. 2011. Nuevo material postcraneano de
1533 *Saurosuchus galilei* Reig (Archosauria: Crurotarsi) del Triasico Superior del centro-oeste
1534 de Argentina. Ameghiniana 48:605-620.
1535 von Baczko, M. B., and J. B. Desojo. 2016. Cranial anatomy and palaeoneurology of the
1536 archosaur *Riojasuchus tenuisceps* from the Los Colorados Formation, La Rioja,
1537 Argentina. PLoS One 11: e0148575
1538 von Baczko, M. B., J. B. Desojo, and D. Pol. 2014. Anatomy and phylogenetic position of
1539 *Venaticosuchus rusconii* Bonaparte, 1970 (Archosauria, Pseudosuchia), from the
1540 Ischigualasto Formation (Late Triassic), La Rioja, Argentina. Journal of Vertebrate
1541 Paleontology 34:1342-1356.
1542 von Baczko, M. B., and M. D. Ezcurra. 2013. Ornithosuchidae: a group of Triassic archosaurs
1543 with a unique ankle joint; pp. 187-202 in S. J. Nesbitt, J. B. Desojo, and R. B. Irmis
1544 (eds.), Anatomy, Phylogeny and Palaeobiology of Early Archosaurs and their Kin.
1545 Geological Society, London, Special Publications, London.

1546 Walker, A. D. 1990. A revision of *Sphenosuchus acutus* Haughton, crocodylomorph reptile from
1547 the Elliot Formation (Late Triassic or Early Jurassic) of South Africa. Philosophical
1548 Transactions of the Royal Society of London B 330:1-120.
1549 Weinbaum, J. C. 2011. The skull of *Postosuchus kirkpatricki* (Archosauria: Paracrocodyliformes)
1550 from the Upper Triassic of the United States. PaleoBios 30:18-44.
1551 Weinbaum, J. C. 2013. Postcranial skeleton of *Postosuchus kirkpatricki* (Archosauria:
1552 Paracrocodylomorpha), from the Upper Triassic of the United States; pp. 525-553 in S.
1553 J. Nesbitt, J. B. Desojo, and R. B. Irmis (eds.), Anatomy, Phylogeny and Palaeobiology
1554 of Early Archosaurs and their Kin. Geological Society, London, Special Publications,
1555 London.
1556 Weinbaum, J. C., and A. Hungerbühler. 2007. A revision of *Poposaurus gracilis* (Archosauria:
1557 Suchia) based on two new specimens from the Late Triassic of the southwestern U.S.A.
1558 Paläontologische Zeitschrift 81/2:131-145.
1559 Witmer, L. M. 1997. The evolution of the antorbital cavity of archosaurs: a study in soft-tissue
1560 reconstruction in the fossil record. Journal of Vertebrate Paleontology Memoir 3:1-73.
1561 Wroblewski, A. F.-J. 1997. Mixed assemblages and the birth of a chimera: an example from the
1562 Popo Agie Formation (Upper Triassic), Wyoming. Journal of Vertebrate Paleontology 17
1563 (suppliment to 3):86A.
1564 Zawiskie, J. M., and R. M. Dawley. 2003. On the skull and holotype of *Heptasuchus clarki*
1565 (Rauisuchia, Poposauridae) from the Upper Triassic Popo Agie Formation, Natrona Co.
1566 Wyoming. Southwest Paleontological Symposium 2003 Guide to Presentations.
1567

1568 Figure Captions

1569 Figure 1. The Triassic System in Wyoming with the location of the type locality of *Heptasuchus*
1570 *clarki*. Stratigraphic section at the type locality of *Heptasuchus clarki* in the upper portion of the

unnamed red beds of the upper portion of the Chugwater Group, Big Horn Mountains and a detailed stratigraphic section through the bonebed. Abbreviations: cm, centimeters, LS, limestone; SS, sandstone. Chugwater Group stratigraphic information from Cavaroc and Flores (1991). [1 column]

Figure 2. The holotype skull of *Heptasuchus clarki* (UW 11562) as found in the field. Drawing by Dawley. Abbreviations: bc, braincase; j, jugal; l., left; mx, maxilla; n, nasal; pmx, premaxilla; po, postorbital; r., right; sp?, splenial?. [1 column]

Figure 3. Reconstruction of the skeleton of *Heptasuchus clarki* in lateral view illustrating the material recovered from the type locality. Skeleton reconstruction based on *Postosuchus kirkpatricki* (Nesbitt et al. 2013) and skull reconstruction based on Gower (1999). Scale = 50 cm. [2 columns]

Figure 4. Skull elements of *Heptasuchus clarki* (UW 11562): left maxilla (UW 11562-C) in lateral (A) and medial (B) views; right maxilla (UW 11562-B) in medial (C) and lateral (D) views; right premaxilla (UW 11562-A) in lateral (E) and medial (F) views; right nasal (UW 11562-F) in lateral (G) and medial (H) views. Abbreviations: a., articulates with; al, alveolus; anf, antorbital fenestra; anfo, antorbital fossa; d, depression; dp, dorsal process; en, external naris; f, fossa; for, foramen; fr, frontal; j, jugal; la, lacrimal; ms, midline suture; mx, maxilla; nf, narial fossa; pd, posterodorsal process; plp, palatal process of the premaxilla; plm, palatal process of the maxilla; pmx, premaxilla; r, ridge; rt, replacement tooth; t, tooth; tr, tooth root. Broken surfaces indicated in hash marks. Scales = 5 cm. [2 columns]

Figure 5. Skull elements of *Heptasuchus clarki* (UW 11562): right postorbital (UW 11562-G) in dorsal (A), medial (B) and lateral (C) views; right jugal (UW 11562-D) in lateral (D) and medial

(E) views; left palatine (UW 11562-K) in dorsal (F) view. Abbreviations: a., articulates with; d, depression; ec, ectopterygoid; f, fossa; fr, frontal; g, groove; la, lacrimal; ltf, lower temporal fenestra; mx, maxilla; o, orbit; pa, parietal; pf, postfrontal; po, postorbital; prf; prefrontal; sqm squamosal; r, ridge; utf; upper temporal fenestra. Broken surfaces indicated in hash marks. Scales = 5 cm. [2 columns]

Figure 6. The braincase of *Heptasuchus clarki* (UW 11562-H) in right lateral (A), posterolateral (B), medial (C) and posterior (D) views. Abbreviations: bt, basitubera; bpt, basipterygoid process; ci, crista interfenestralis; cp, cultriform process; f, fossa; fo, fenestra ovalis; g., groove for; ic, entrance of the internal carotid; lr, lateral ridge; mf, metotic foramen; np, notochoral pit; oc, occipital condyle; pa, parietal; pbs, parabasisphenoid; pp, paroccipital process of the otoccipital; ppt; ridge possibly for attachment of protractor pterygoidei; ptf, posttemporal fenestra; so, supraoccipital; ug, unossified gap; V, exit of cranial nerve V (trigeminal); VI, exit of cranial nerve VI (abducens);VII, exit of cranial nerve V (facial); XII, exit of cranial nerve XII (hypoglossal). Broken surfaces indicated in hash marks. Scales = 5 cm. [2 columns]

Figure 7. Fragmentary skull elements of *Heptasuchus clarki:* ventral portion of the left quadrate (UW 11563-AF + UW 11563-H, labeled before putting together) in posterior (A), anterior (B), and ventral (C) views; dorsal head of the quadrate (side unknown; UW 11562) in lateral? (D) view; possible fragments of the pterygoid (UW 11562-M) in two (E-F) views; possible fragment of the pterygoid (UW 11562-L) in two (G-H) views. Scales = 1 cm. [1 column]

Figure 8. Axial elements of *Heptasuchus clarki*: posterior trunk vertebra (TMM unnumbered) in right lateral (A) and posterior (B) views; neural spine of a cervical-trunk vertebra (UW ll562-CX) in dorsal (C) and posterior (D) views; presacral neural spine (UW ll562-V) in lateral (E) view; presacral neural spine (UW ll562-CT) in lateral (F) view; anterior caudal vertebra in lateral (G)

and anterior (H) views; distal caudal vertebra (UW 11562-BW) in ventral (I) and posterior (J) views; osteoderm (TMM unnumbered) in three views; anterior caudal vertebra in dorsal (K), medial (L), and lateral (M) views. Scales = 1 cm. [1 column]

Figure 9. Pectoral elements and partial humerus of *Heptasuchus clarki*: right partial scapula (UW 11565-E) in lateral (A) view; partial left coracoid (UW 11566) in lateral (B) view; proximal portion of left humerus (UW 11565-A) in proximal (C) and posterior (D) views. Abbreviations: cf, coracoid foramen; dp, deltopectoral crest; gl, glenoid; tu, tuber. Scales = 1 cm. [1 column]

Figure 10. Forelimb elements of *Heptasuchus clarki*: proximal portion of the radius (UW 11562-DM) in proximal (A), and lateral (B) views and the distal portion of the radius (UW 11562-DI) in ?anterior (C) and distal (D) views; right ulna (UW 11562-W) in proximal (E), medial (F), posterior (G), and distal (H) views; left ulna in (UW 11562-X) in proximal (I), posterior (J), anterior (K), and distal (L) views. Scales = 1 cm in A-D and 5 cm in E-L. [1 column]

Figure 11. Pelvic elements of *Heptasuchus clarki*: left pubis (UW 11562-Y) in lateral (A), anterior (B), medial (C), and distal (B) views; proximal portion of the right ischium (UW 11564-B) in lateral (E) view; pubic peduncle of the right ilium (UW 11563) in lateral (F) view. Abbreviations: a., articulates with; as, acetabulum; il, ilium; pa, pubic apron; pb, pubic boot; pp, pubic peduncle; pu, pubis; Scales = 5 cm in A-B and 1 cm in E-F. [1 column]

Figure 12. Hindlimb elements of *Heptasuchus clarki*: proximal portion of a right femur (UW 11563-B) in proximal (A) and anterolateral (B) views and the distal portion of the right femur (UW 11563-A) in anterior (C) and distal (D) views; left tibia (UW 11562-Z) in proximal (E), posterior (F), anterior (G), and distal (H) views; proximal portion of a right fibula (UW 11566-S)

in proximal (I) and anterolateral (J) views and the distal portion of the right fibula (UW 11566-R) in anterior (K) and distal (L) views. Scales = 1 cm in A-D, I-L and = 5 cm in E-H. [1 column]

Figure 13. Partial phylogenetic tree focused on pseudosuchian relationships with *Heptasuchus clarki* included. *Heptasuchus clarki* was found as a loricatan as the sister-taxon of *Batrachotomus kuperferzellensis*. Tree derived from 72 most parsimonious trees (MPTs) of length (1529 steps) (Consistency Index = 0.335; Retention Index = 0.752)(see supplemental information figure S2). [1 column]

Figure 14. New illustrated character states for paracrocodylomorph archosaurs: (A) skull referred to *Prestosuchus chiniquensis* (ULBRA-PVT-281) in right lateral view; (B) right postorbital of *Batrachotomus kuperferzellensis* (SMNS 52970) in dorsal (top) and lateral (bottom) view; (C) left postorbital of *Heptasuchus clarki* (UW 11562) in lateral view; (D) left maxilla of *Batrachotomus kuperferzellensis* (SMNS 52970) in medial view; (E) right maxilla of *Heptasuchus clarki* (UW 11562) in medial view; (F) right nasal of *Batrachotomus kuperferzellensis* (SMNS 52970) in lateral view; (G) right nasal of *Heptasuchus clarki* (UW 11562) in lateral view; (H) left maxilla of *Xilousuchus sapingensis* (IVPP V6026) in medial view; (I) right premaxilla of *Heptasuchus clarki* (UW 11562) in lateral view; (J) left premaxilla of *Postosuchus kirkpatricki* (TTUP 9000) in lateral view; (K) left premaxilla of *Xilousuchus sapingensis* (IVPP V6026) in lateral view; (L) right jugal of *Heptasuchus clarki* (UW 11562) in lateral view; (M) right jugal of *Heptasuchus clarki* (UW 11562) in medial view; (N) left jugal of *Batrachotomus kuperferzellensis* (SMNS 52970) in lateral view; (O) left jugal of *Batrachotomus kuperferzellensis* (SMNS 52970) in medial view. Numbers refer to character number separated by a dash from the state. Scales in 10 cm in A, 5 cm in C-G, I, L-M, and 1 cm in B, H, J-K, N-O. [2 columns]

Appendix: New character descriptions and illustrations:

425. Postorbital, ventral end, depression on the anterolateral surface: (0) - absent; (1) - present. (new; Fig. 14)

The plesiomorphic condition, state 0, in stem archosaurs and within Archosauria is to have a tapering ventral end of the postorbital that fits onto the anterodorsal edge of the dorsal process of the jugal and this condition is clear in the following exemplary taxa: *Euparkeria capensis* (Ewer 1965); *Lewisuchus admixtus* (Bittencourt et al. 2014); *Gracilisuchus stipanicicorum* (MCZ 4117), *Paratypothorax andressorum* (SMNS 19003; Schoch and Desojo 2015) and *Luperosuchus fractus* (PULR 04). In a number of loricatan taxa (e.g., *Postosuchus kirkpatricki*, TTUP 9000; *Batrachotomus kupferzellensis*, SMNS 80260; *Heptasuchus clarki*, UW 11562), the ventral end of the postorbital extends anteriorly into the orbit (Benton and Clark 1988; Juul, 1994; Benton, 1999; Alcober, 2000; Benton and Walker, 2002; Brusatte et al. 2010; Nesbitt 2011 Character 65). Out of these taxa, the ventral end of the postorbital is flat or nearly flat whereas a depression on the ventrolateral portion of the distal end of the postorbital is present in both *Batrachotomus kupferzellensis* (SMNS 80260) and *Heptasuchus clarki* (UW 11562) – state 1. Gower (1999) listed the depression as a possible autapomorphy of *Batrachotomus kupferzellensis*. The ventrolateral depression in *Heptasuchus clarki* is much deeper and much of the depth is hidden in lateral view compared to *Batrachotomus kupferzellensis*.

426. Maxilla, medial side, ventral surface of palatal process: (0) flat; (1) - depression present. (new; Fig. 14)

The palatal process of the maxilla is horizontal in most archosauriforms and the ventral surface of the palatal process is typically flat or slightly concave. Within Pseudosuchia, the ventral surface of the palatal process is flat in *Xilousuchus sapingensis* (Nesbitt et al. 2011), *Revueltosaurus callenderi* (PEFO 34561) and in the ornithosuchid *Riojasuchus tenuisceps* (PVL

3827; von Baczko and Desojo 2016). In contrast, a dorsally extended depression at the posteroventral side of the palatal process of the maxilla is present in *Postosuchus kirkpatricki* (TTUP 9000), *Polonosuchus silesiacus* (ZPAL Ab III/543), *Fasolasuchus tenax* (PVL 3851), *Heptasuchus clarki* (UW 11562). *Batrachotomus kupferzellensis* (SMNS 80260), *Arganosuchus dutuit* (ALM 1; Jalil and Peyer 2007) and possibly in *Sphenosuchus actus* (SAM 3014). It appears that the depression is not present in any of the *Prestosuchus chiniquensis* specimens where the palatal process is visible (Mastrantonio et al. 2019). In some taxa (e.g., *Postosuchus kirkpatricki,* TTUP 9000) the depression is much deeper in that the depression extends well dorsal to the dorsal extent of the palatal process whereas in *Sphenosuchus actus*, the depression is rather shallow but occurs in the same position as that of other loricatans. The function of the depression is not clear. Chatterjee (1985) hypothesized that the depression could serve as the area for Jacobson's organ. However, Weinbaum (2011) points out that Jacobson's organ is not present in crocodylians and avians and thus unlikely that this depression was for housing Jacobson's organ. The depression is located too far medially and, in most taxa, dorsally to represent a depression for accepting an enlarged dentary tooth.

427. Postorbital, lateral side, posterodorsal portion of the ventral process: (0) – smooth; (1) – slight depression, usually ventral to a rounded knob or ridge. (new; Fig. 14)

The posterior side of the postorbital is typically bowed or flat similar to the anterior and lateral sides of the base of the ventral process. Examples of taxa with this plesiomorphic condition include *Euparkeria capensis* (Ewer 1965); *Lewisuchus admixtus* (Bittencourt et al. 2014); *Gracilisuchus stipanicicorum* (MCZ 4117), and *Paratypothorax andressorum* (SMNS 19003; Schoch and Desojo 2015). Within Paracrocodylomorpha, *Luperosuchus fractus* (PULR 04), and *Xilousuchus sapingensis* (Nesbitt et al. 2011) have state 0. In *Prestosuchus chiniquensis* (UFRGS-PV-0629-T; Mastrantonio et al. 2019), *Postosuchus kirkpatricki* (TTUP 9000), *Batrachotomus kupferzellensis* (SMNS 80260), *Heptasuchus clarki* (UW 11562),

Arizonasaurus babbitti (MSM 4590), and *Sphenosuchus actus* (SAM 3014) have a clear depression on the posterior side of the ventral process of the postorbital near its base (i.e., near the contact with the squamosal. The taxa scored as state 1 typically have a vertical ridge, sometimes rugose, that divide the anterior part of the ventral process of the postorbital from the posterior portion.

428. Squamosal - postorbital articulation: (0) - postorbital fits into a groove on the lateral side of the squamosal; (1) - the postorbital lies on the dorsal surface of the squamosal; (2) - the squamosal largely lies on the dorsal surface of the postorbital. (new; Fig. 14)

In stem archosaurs and most members of Archosauria, the posterior portion of the postorbital fits into a clear slot into the lateral side of the squamosal. Clear examples of this articulation include *Euparkeria capensis* (Ewer 1965), *Arizonasaurus babbitti* (MSM 4590), *Paratypothorax andressorum* (SMNS 19003; Schoch and Desojo 2015), and *Riojasuchus tenuisceps* (PVL 3827; von Baczko and Desojo 2016). In most loricatans, the anterior process of the squamosal largely fits on the dorsal surface of the postorbital (state 1). As noted by Gower (1999) for *Batrachotomus kupferzellensis*, much of the squamosal of the taxon dorsally overlaps the postorbital, but there is some complexity to this articulation; a small part of the posteromedial portion of the postorbital is underlapped by the squamosal, and this results in the postorbital lying in a small notch of the squamosal. Early diverging loricatans *Luperosuchus fractus* (Nesbitt and Desojo 2017), *Prestosuchus chiniquensis* (UFRGS-PV-0629-T), and *Saurosuchus galilei* (PVSJ 32) appear to have state 1, although it is a bit difficult to see the articulation in the specimens represented by partially articulated or fully articulated skulls. State 1 is clearly present in *Batrachotomus kupferzellensis* (SMNS 80260), *Heptasuchus clarki* (UW 11562), and *Postosuchus kirkpatricki* (TTUP 9000). Within Crocodylomorpha, state 2 appears to be present across the clade where the postorbital largely lies over the squamosal and this is clear in early members of crocodylomorphs like *Dromicosuchus grallator* (NCSM 13733),

Dibothrosuchus elaphros (IVPP V 7907), and *Litargosuchus leptorhynchus* (Clark and Sues 2002). Crocodyliforms appear to have an interdigitating suture between the postorbital and squamosal so these taxa are scored as ?.

429. Jugal, posterior process, medial side, longitudinal groove: (0) – absent; (1) - present. (new; Fig. 14)

Typically, the medial surface of the posterior process of the jugal of stem archosaurs (e.g., *Euparkeria capensis*) and members of Archosauria (e.g., *Arizonasaurus babbitti*, MSM 4590; *Effigia okeeffeae*; Nesbitt, 2007) are smooth. A clear groove, that parallels the ventral edge is present for nearly the entire length of the jugal in *Batrachotomus kuperferzellensis* (SMNS 52970), *Postosuchus kirkpatricki* (TTUP 9000), *Polonosuchus silesiacus* (ZPAL Ab III/543), *Heptasuchus clarki* (UW 11562), and *Sphenosuchus actus* (SAM 3014).

430. Nasal, posterodorsal corner of the naris: (0) - smooth or slight fossa; (1) - distinct fossa with a rim present. (new; Fig. 14)

The anterior portion of the nasal of archosaurs typically splits into a process that lies dorsal to the external naris and one that extends anteroventrally posterior of the external naris (=descending process of some). In the juncture of the two anterior processes, the surface is typically flat. This is the case in most loricatans (e.g., *Postosuchus kirkpatricki*; TTUP 9000; specimens referred to *Prestosuchus chiniquensis*). In *Batrachotomus kuperferzellensis* (SMNS 52970) and *Heptasuchus clarki* (UW 11562), there is a clear narial fossa (sensu Gower 1999) between the two anterior processes. Ventral to this fossa, a ridge framing the fossa is present on the anteroventral process in these taxa. This depression is not the fully the consequence of the ridge present dorsally (character 35, state 1) given that *Postosuchus kirkpatricki* (TTUP 9000) possesses that ridge, but not the fossa. A Moenkopi form (NMMNH 55779; Schoch et al. 2010) also possesses state 1.

1778

1779 431. Maxilla, anteroventral corner: (0) - abuts premaxilla; (1) - extensively laterally overlaps the
1780 posteroventral corner of the premaxilla. (new; Fig. 14)

1781 Within stem archosaurs and within Archosauria, the juncture between the maxilla and
1782 premaxilla at their ventral borders is either separated by a gap (e.g., *Riojasuchus tenuisceps*,
1783 von Baczko and Desojo 2016; *Coelophysis bauri*, Colbert 1989), or is loosely connected (e.g.,
1784 *Euparkeria capensis*, Ewer 1965; *Turfanosuchus dabanensis*, IVPP V3237). In loricatans, there
1785 is a medially extended articulation surface between the maxilla and premaxilla. Here, the
1786 anterolateral portion of the maxilla lies onto a clear articulation surface on the posterolateral side
1787 of the premaxilla. This character state (1) is present in *Saurosuchus galilei* (PVSJ 32),
1788 *Batrachotomus kuperferzellensis* (SMNS 52970), *Heptasuchus clarki* (UW 11562),
1789 *Polonosuchus silesiacus* (ZPAL Ab III/543), and *Fasolasuchus tenax* (PVL 3851). The state in
1790 crocodylomorphs is not clear.

1791 This character is difficult to score in articulated skull because the targeted surfaces
1792 cannot be seen so we recommend only scoring the character if the maxilla and maxilla are
1793 disarticulated and the anterior and of the maxilla is complete. Fine surface preservation is
1794 typically required also. Additionally, it is possible that this character is correlated with larger
1795 sizes; that is, it is easier to see in larger specimens.

1796

1797 432. Premaxilla, base of the posterodorsal process (maxillary process): (0) - flat with the body of
1798 the premaxilla; (1) - laterally bulging from the main body. (new; Fig. 14)

1799 The base of the posterodorsal process of the premaxilla is typically continuous with the
1800 lateral surface of the body of the premaxilla in stem archosaurs (e.g., *Euparkeria capensis*,
1801 Ewer 1965; *Erythrosuchus africanus*, BPI 4526). Within Archosauria, state 0 is typical of
1802 avemetatarsalians (e.g., *Silesaurus opolensis*; Dzik 2003; *Coelophysis bauri*, Colbert 1989) and
1803 occurs throughout early diverging Pseudosuchia (e.g., *Xilousuchus sapingensis*, IVPP V6026;

Paratypothorax andressorum, SMNS 19003; *Riojasuchus tenuisceps*, PVL 3827). In Loricata, *Prestosuchus chiniquensis* (ULBRA-PVT-281), *Saurosuchus galilei* (PVSJ 32), *Heptasuchus clarki* (UW 11562), *Postosuchus kirkpatricki* (TTUP 9000), *Fasolasuchus tenax* (PVL 3850), and *Polonosuchus silesiacus* (ZPAL Ab III/543) all have laterally expanded base of the posterodorsal process of the premaxilla. The bulge is much clearer in some taxa (e.g., *Postosuchus kirkpatricki* TTUP 9000) than others (e.g., *Saurosuchus galilei,* PVSJ 32). Early crocodylomorphs (e.g., *Dromicosuchus grallator,* NCSM 13733) appear to also have state 1.

433. Jugal, lateral surface, anteroposteriorly trending ridge: (0) - symmetrical dorsoventrally; (1) - asymmetrical dorsoventrally where the dorsal portion is more laterally expanded. (new; Fig. 14)

The lateral surface of the jugal of archosaurs is either smooth or bears a ridge that parallels the ventral edge (character 75 of Nesbitt, 2011). The form of the ridge varies across Archosauria and can be a sharp ridge, broad, or laterally extended with as a rugose and broad ridge. Most loricatans have some kind of ridge, but *Heptasuchus clarki* (UW 11562) and *Batrachotomus kuperferzellensis* (SMNS 52970) share a clear expanded ridge that is asymmetrical dorsoventrally where the dorsal portion is more laterally expanded.
Taxa without ridges on the lateral side of the jugal (taxa scored as 75-0) are scored as inapplicable (-) for this character.

Figure 1

The Triassic System in Wyoming with the location of the type locality of *Heptasuchus clarki*

Stratigraphic section at the type locality of *Heptasuchus clarki* in the upper portion of the unnamed red beds of the upper portion of the Chugwater Group, Big Horn Mountains and a detailed stratigraphic section through the bonebed. Abbreviations: cm, centimeters, LS, limestone; SS, sandstone. Chugwater Group stratigraphic information from Cavaroc and Flores (1991).

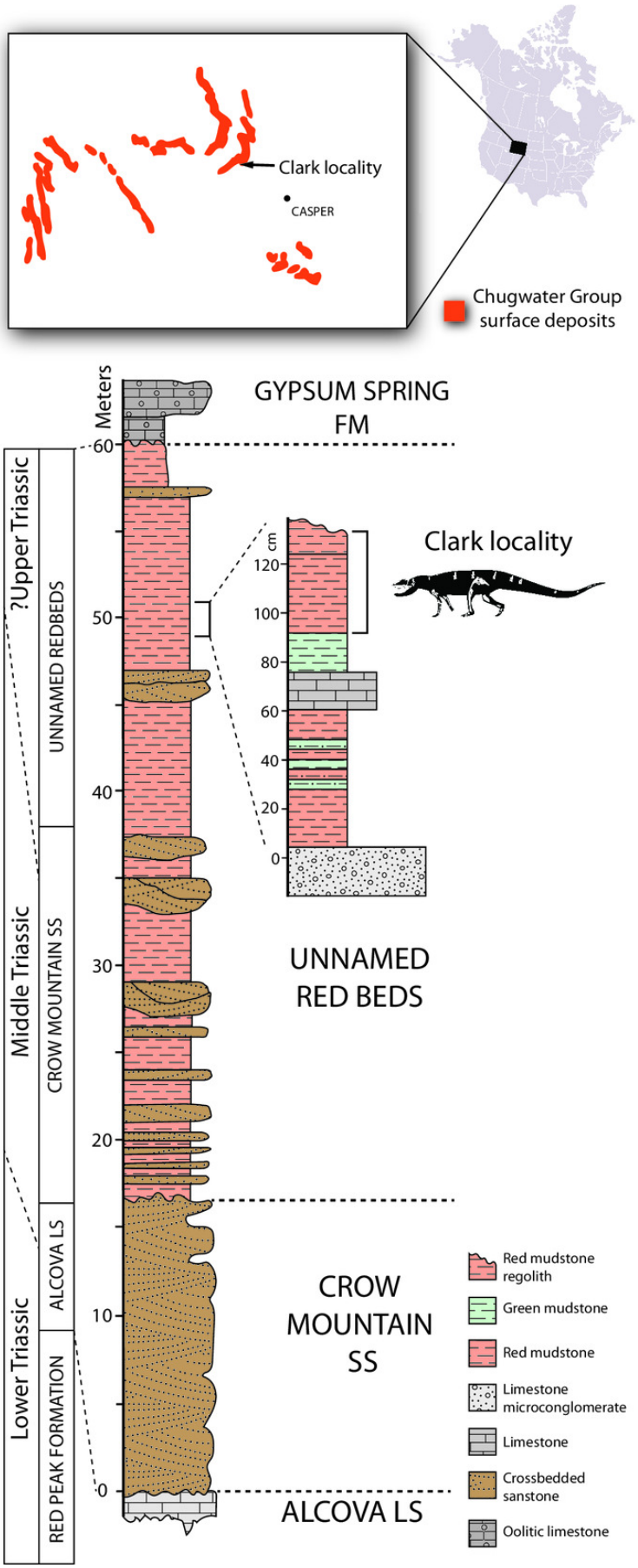
Clark locality
CASPER
Chugwater Group surface deposits
Meters
GYPSUM SPRING FM
Clark locality
cm
120
100
80
60
40
20
0
UNNAMED RED BEDS
CROW MOUNTAIN SS
ALCOVA LS
?Upper Triassic
Middle Triassic
Lower Triassic
UNNAMED REDBEDS
CROW MOUNTAIN SS
ALCOVA LS
RED PEAK FORMATION
60
50
40
30
20
10
0
Red mudstone regolith
Green mudstone
Red mudstone
Limestone microconglomerate
Limestone
Crossbedded sanstone
Oolitic limestone

Figure 2

The holotype skull of *Heptasuchus clarki* (UW 11562) as found in the field. Drawing by Dawley.

Abbreviations: bc, braincase; j, jugal; l., left; mx, maxilla; n, nasal; pmx, premaxilla; po, postorbital; r., right; sp?, splenial?.

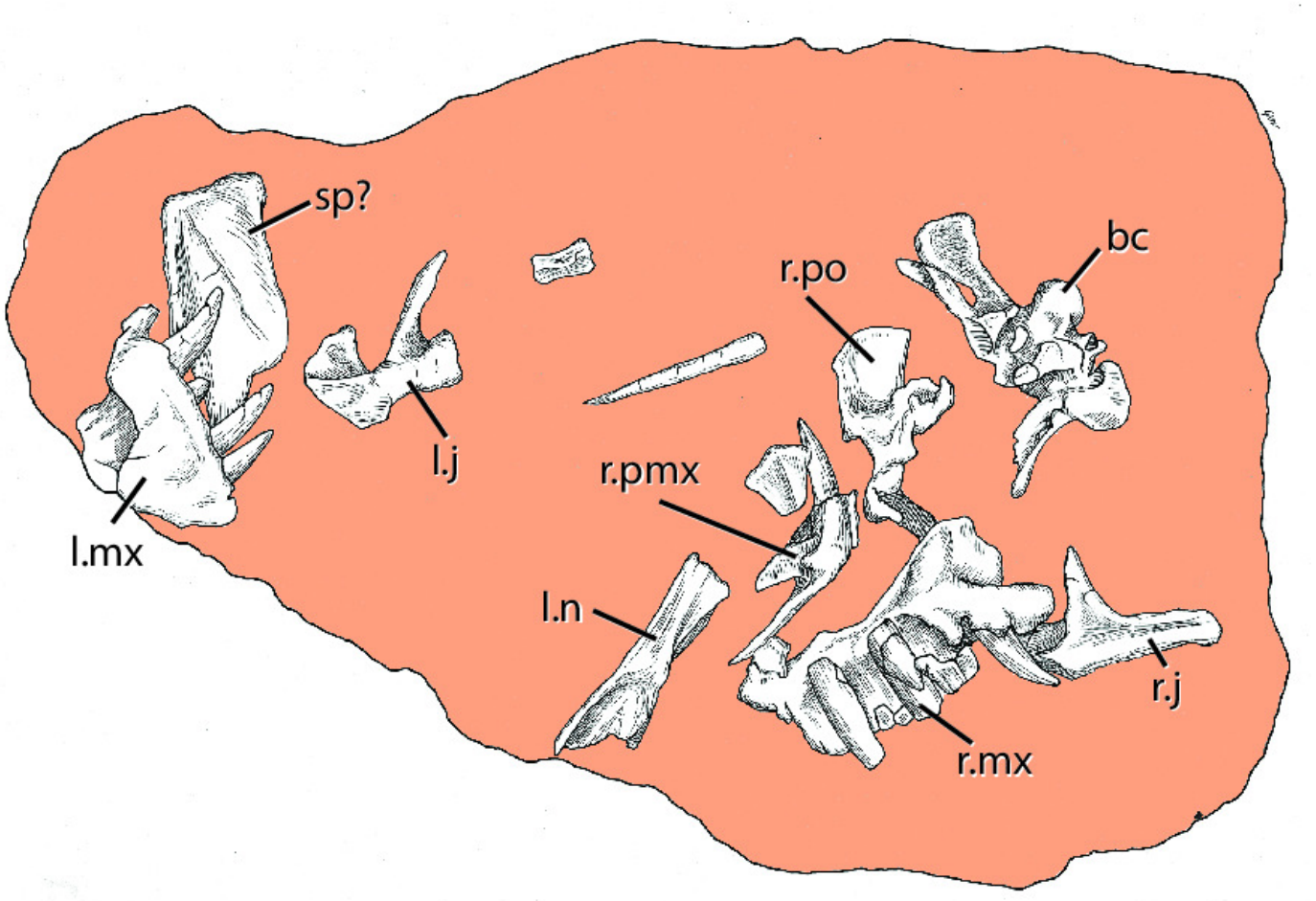

Figure 3

Reconstruction of the skeleton of *Heptasuchus clarki* in lateral view illustrating the material recovered from the type locality.

Skeleton reconstruction based on *Postosuchus kirkpatricki* (Nesbitt et al. 2013) and skull reconstruction based on Gower (1999). Scale = 50 cm.

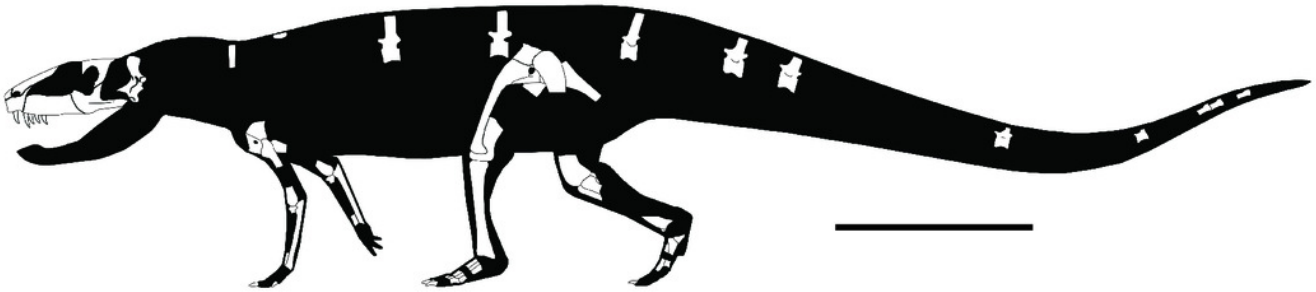

Figure 4

Skull elements of *Heptasuchus clarki* (UW 11562):

left maxilla (UW 11562-C) in lateral (A) and medial (B) views; right maxilla (UW 11562-B) in medial (C) and lateral (D) views; right premaxilla (UW 11562-A) in lateral (E) and medial (F) views; right nasal (UW 11562-F) in lateral (G) and medial (H) views. Abbreviations: a., articulates with; al, alveolus; anf, antorbital fenestra; anfo, antorbital fossa; d, depression; dp, dorsal process; en, external naris; f, fossa; for, foramen; fr, frontal; j, jugal; la, lacrimal; ms, midline suture; mx, maxilla; nf, narial fossa; pd, posterodorsal process; plp, palatal process of the premaxilla; plm, palatal process of the maxilla; pmx, premaxilla; r, ridge; rt, replacement tooth; t, tooth; tr, tooth root. Broken surfaces indicated in hash marks. Scales = 5 cm.

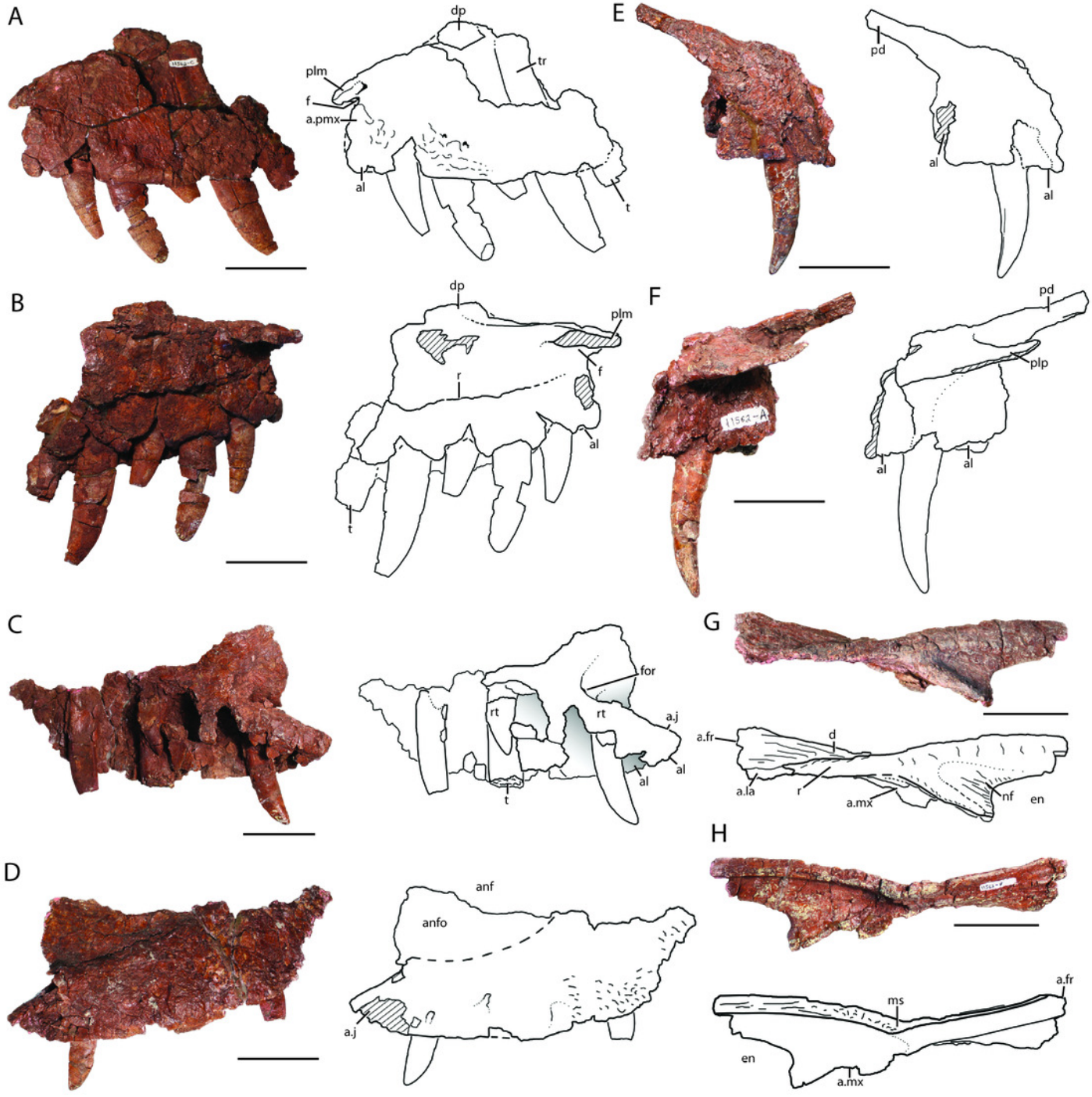
A
dp
plm
f
a.pmx
tr
al
t
E
pd
al
al
B
dp
plm
f
r
al
t
F
pd
plp
al
al
C
for
rt
rt
a.j
al
al
t
G
a.fr
d
a.la
r
a.mx
nf
en
D
anf
anfo
a.j
H
a.fr
ms
en
a.mx

Figure 5

Skull elements of *Heptasuchus clarki* (UW 11562):

right postorbital (UW 11562-G) in dorsal (A), medial (B) and lateral (C) views; right jugal (UW 11562-D) in lateral (D) and medial (E) views; left palatine (UW 11562-K) in dorsal (F) view. Abbreviations: a., articulates with; d, depression; ec, ectopterygoid; f, fossa; fr, frontal; g, groove; la, lacrimal; ltf, lower temporal fenestra; mx, maxilla; o, orbit; pa, parietal; pf, postfrontal; po, postorbital; prf; prefrontal; sqm squamosal; r, ridge; utf; upper temporal fenestra. Broken surfaces indicated in hash marks. Scales = 5 cm.

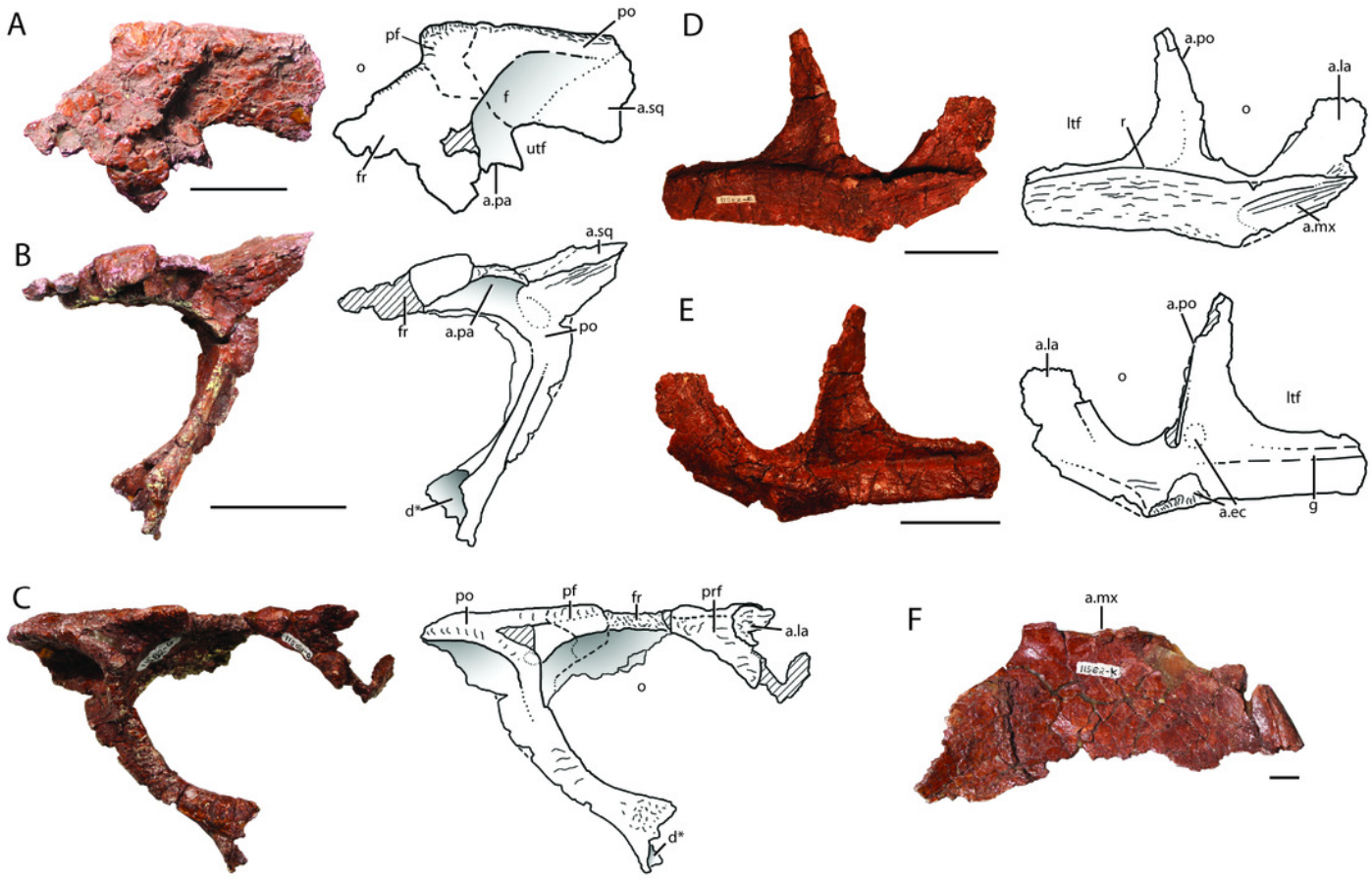

Figure 6

The braincase of *Heptasuchus clarki* (UW 11562-H) in right lateral (A), posterolateral (B), medial (C) and posterior (D) views.

Abbreviations: bt, basitubera; bpt, basipterygoid process; ci, crista interfenestralis; cp, cultriform process; f, fossa; fo, fenestra ovalis; g., groove for; ic, entrance of the internal carotid; lr, lateral ridge; mf, metotic foramen; np, notochoral pit; oc, occipital condyle; pa, parietal; pbs, parabasisphenoid; pp, paroccipital process of the otoccipital; ppt; ridge possibly for attachment of protractor pterygoidei; ptf, posttemporal fenestra; so, supraoccipital; ug, unossified gap; V, exit of cranial nerve V (trigeminal); VI, exit of cranial nerve VI (abducens);VII, exit of cranial nerve V (facial); XII, exit of cranial nerve XII (hypoglossal). Broken surfaces indicated in hash marks. Scales = 5 cm.

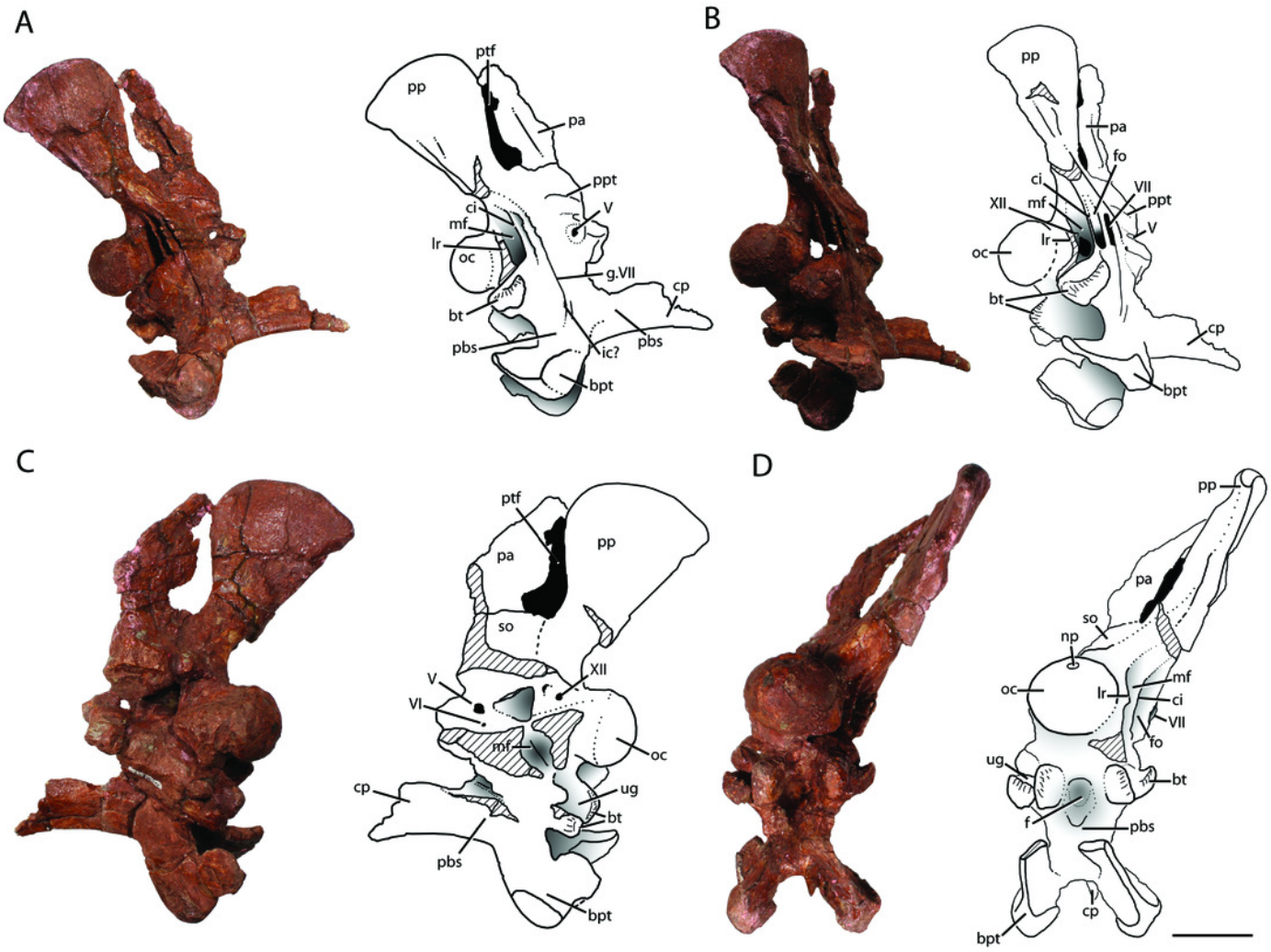
A
ptf
pp
pa
ppt
V
ci
mf
lr
oc
g.VII
cp
bt
pbs
ic?
pbs
bpt
B
pp
pa
fo
ci
VII
XII
mf
ppt
V
lr
oc
bt
cp
bpt
C
ptf
pp
pa
so
XII
V
VI
mf
oc
cp
ug
bt
pbs
bpt
D
pp
pa
so
np
oc
lr
mf
ci
VII
fo
ug
bt
f
pbs
cp
bpt

Figure 7

Fragmentary skull elements of *Heptasuchus clarki:*

ventral portion of the left quadrate (UW 11563-AF + UW 11563-H, labeled before putting together) in posterior (A), anterior (B), and ventral (C) views; dorsal head of the quadrate (side unknown; UW 11562) in lateral? (D) view; possible fragments of the pterygoid (UW 11562-M) in two (E-F) views; possible fragment of the pterygoid (UW 11562-L) in two (G-H) views. Scales = 1 cm.

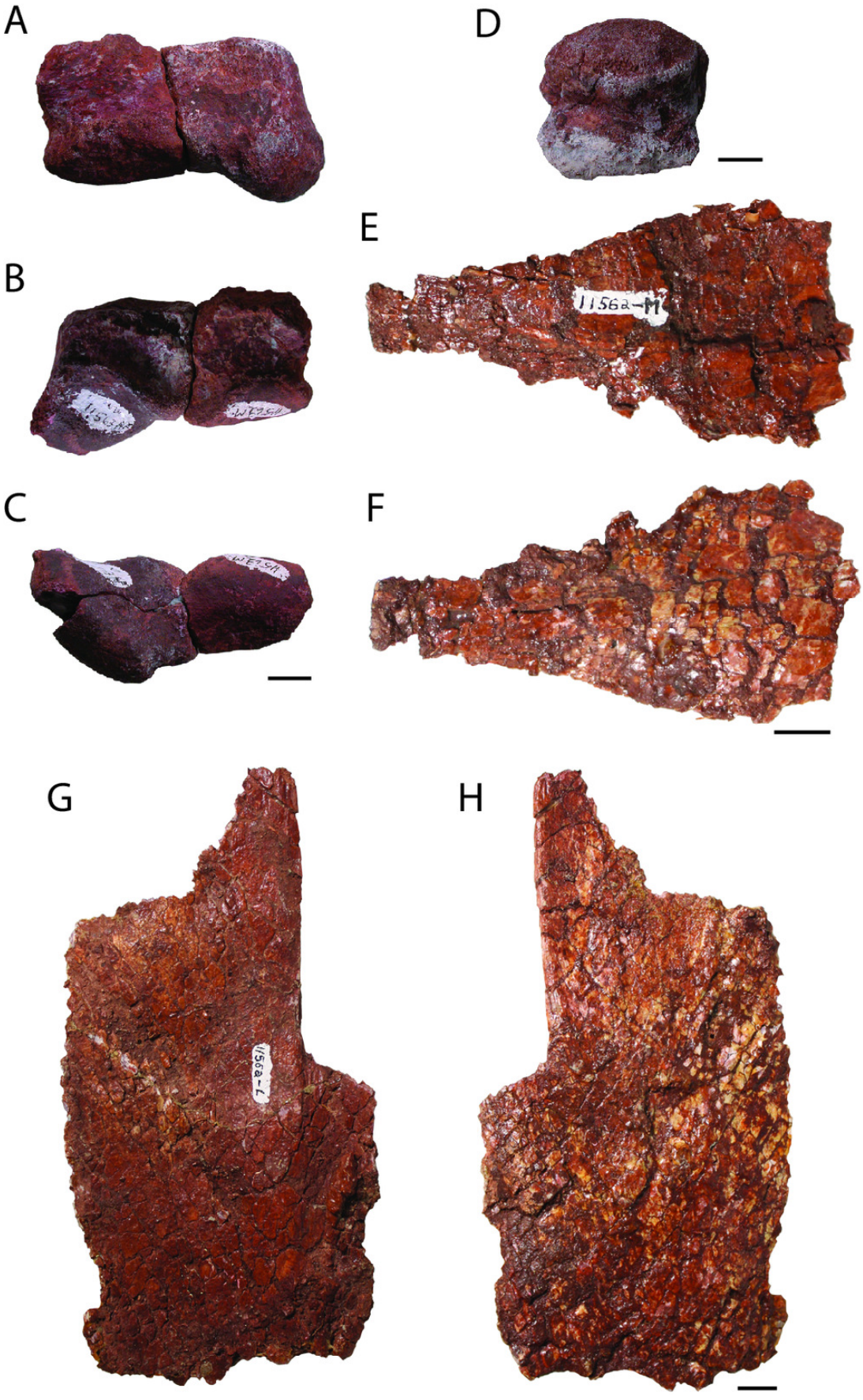
A
D
E
B
11562-M
C
F
G
H

Figure 8

Axial elements of *Heptasuchus clarki*:

posterior trunk vertebra (TMM unnumbered) in right lateral (A) and posterior (B) views; neural spine of a cervical-trunk vertebra (UW ll562-CX) in dorsal (C) and posterior (D) views; presacral neural spine (UW ll562-V) in lateral (E) view; presacral neural spine (UW ll562-CT) in lateral (F) view; anterior caudal vertebra in lateral (G) and anterior (H) views; distal caudal vertebra (UW 11562-BW) in ventral (I) and posterior (J) views; osteoderm (TMM unnumbered) in three views; anterior caudal vertebra in dorsal (K), medial (L), and lateral (M) views. Scales = 1 cm.

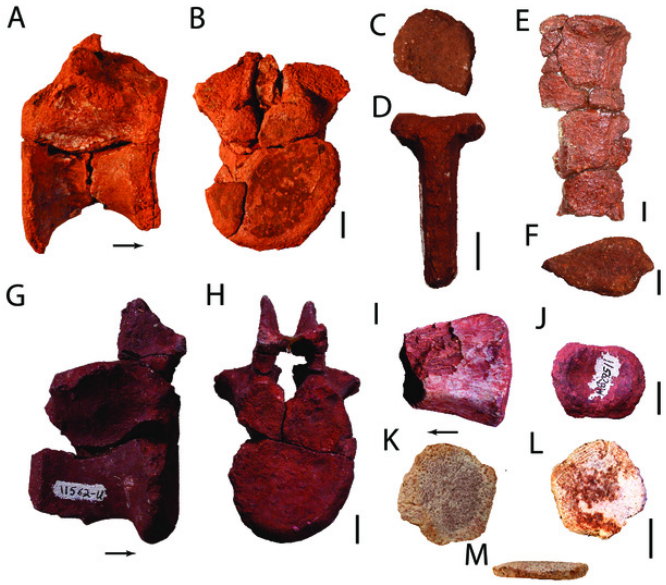
A
B
C
D
E
F
G
H
I
J
K
L
M

Figure 9

Pectoral elements and partial humerus of *Heptasuchus clarki*:

right partial scapula (UW 11565-E) in lateral (A) view; partial left coracoid (UW 11566) in lateral (B) view; proximal portion of left humerus (UW 11565-A) in proximal (C) and posterior (D) views. Abbreviations: cf, coracoid foramen; dp, deltopectoral crest; gl, glenoid; tu, tuber. Scales = 1 cm.

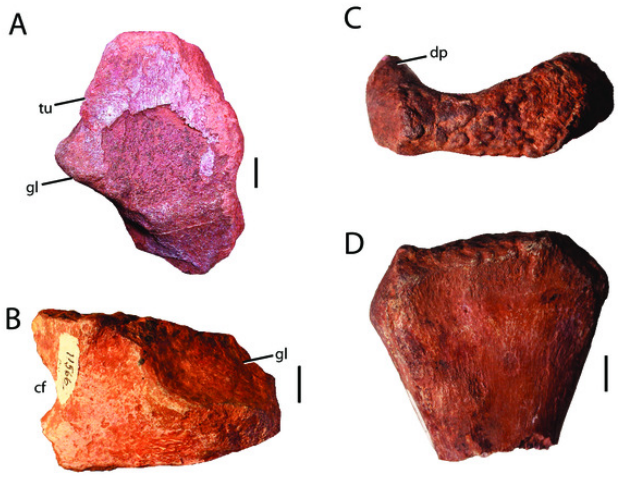
A
tu
gl
B
gl
cf
C
dp
D

Figure 10

Forelimb elements of *Heptasuchus clarki*:

proximal portion of the radius (UW 11562-DM) in proximal (A), and lateral (B) views and the distal portion of the radius (UW 11562-DI) in ?anterior (C) and distal (D) views; right ulna (UW 11562-W) in proximal (E), medial (F), posterior (G), and distal (H) views; left ulna in (UW 11562-X) in proximal (I), posterior (J), anterior (K), and distal (L) views. Scales = 1 cm in A-D and 5 cm in E-L.

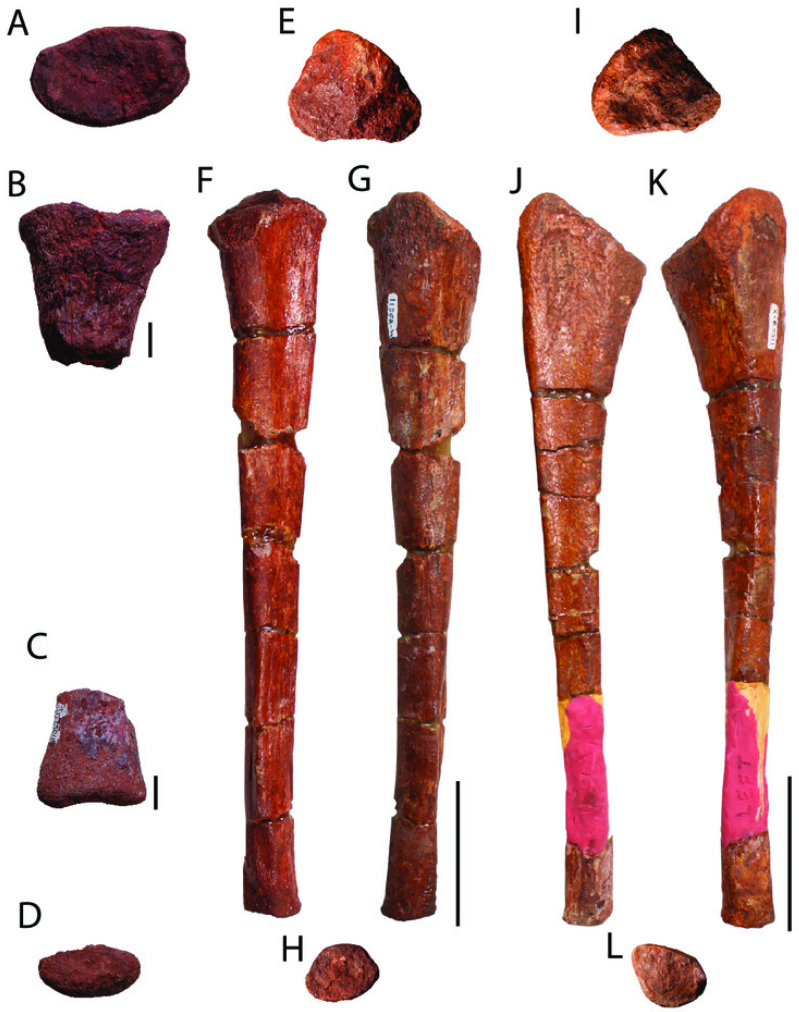
A
E
I
B
F
G
J
K
C
D
H
L

Figure 11

Pelvic elements of *Heptasuchus clarki*:

left pubis (UW 11562-Y) in lateral (A), anterior (B), medial (C), and distal (B) views; proximal portion of the right ischium (UW 11564-B) in lateral (E) view; pubic peduncle of the right ilium (UW 11563) in lateral (F) view. Abbreviations: a., articulates with; as, acetabulum; il, ilium; pa, pubic apron; pb, pubic boot; pp, pubic peduncle; pu, pubis; Scales = 5 cm in A-B and 1 cm in E-F.

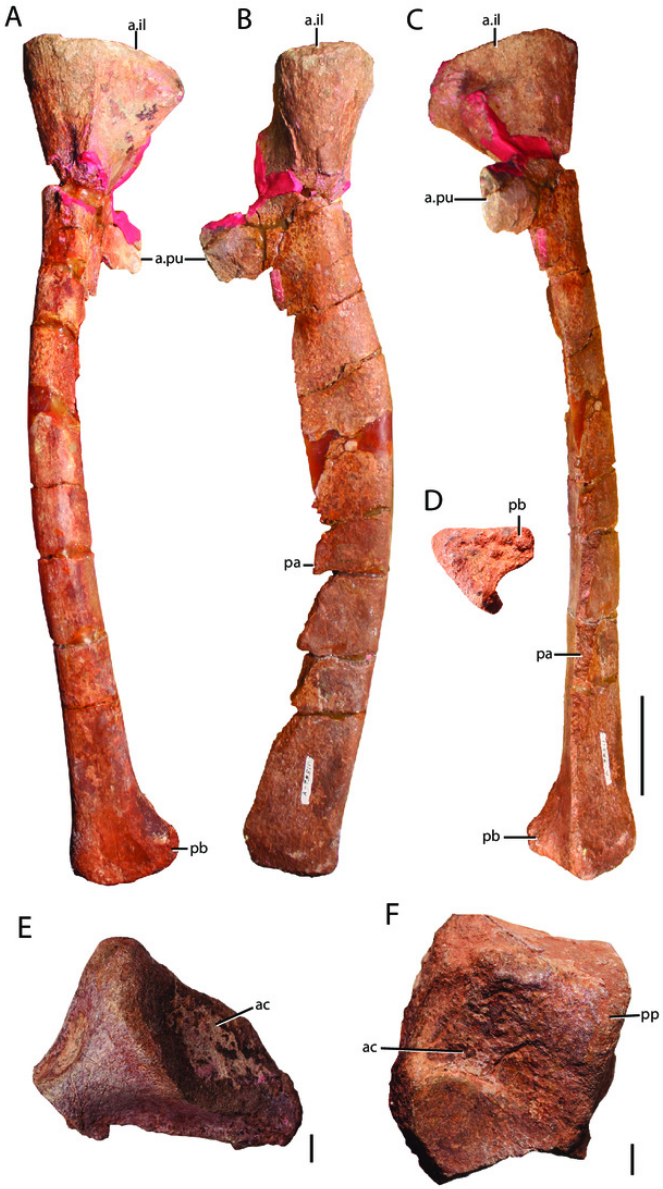
A
a.il
a.pu
pb
B
a.il
pa
C
a.il
a.pu
D
pb
pa
pb
E
ac
F
pp
ac

Figure 12

Hindlimb elements of *Heptasuchus clarki*:

proximal portion of a right femur (UW 11563-B) in proximal (A) and anterolateral (B) views and the distal portion of the right femur (UW 11563-A) in anterior (C) and distal (D) views; left tibia (UW 11562-Z) in proximal (E), posterior (F), anterior (G), and distal (H) views; proximal portion of a right fibula (UW 11566-S) in proximal (I) and anterolateral (J) views and the distal portion of the right fibula (UW 11566-R) in anterior (K) and distal (L) views. Scales = 1 cm in A-D, I-L and = 5 cm in E-H.

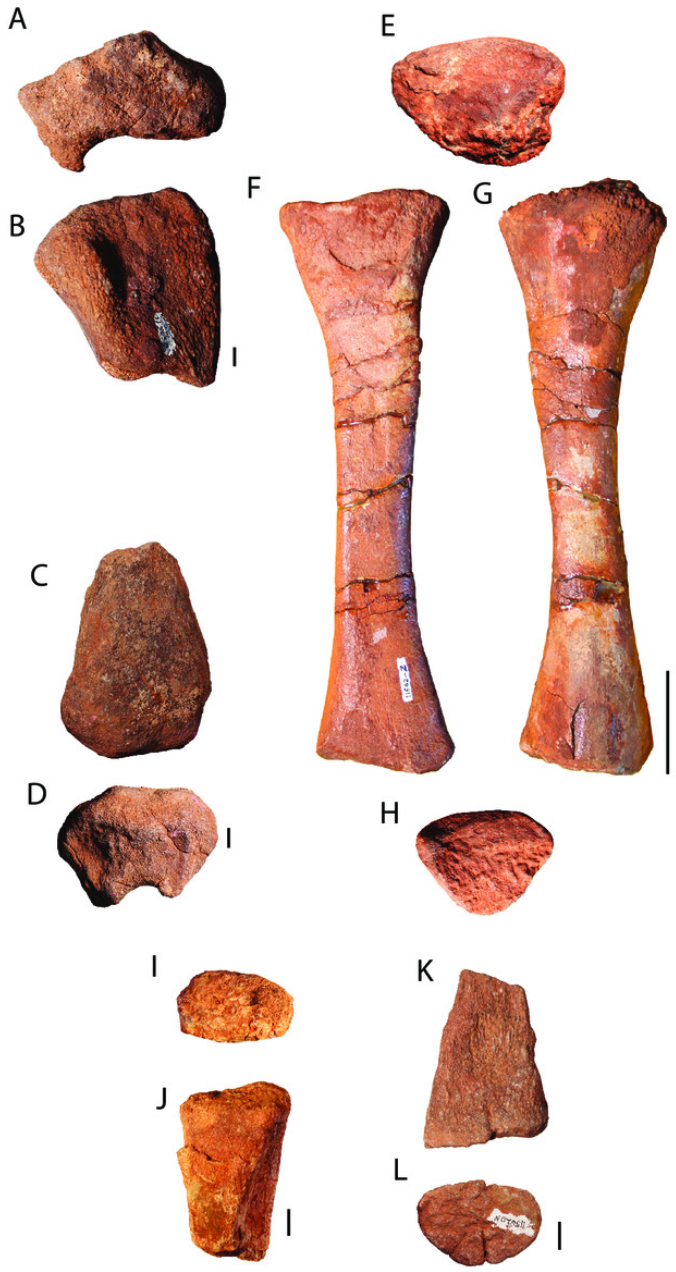
A
E
B
F
G
I
C
D
I
H
I
K
J
I
L
I

Figure 13

Partial phylogenetic tree focused on pseudosuchian relationships with *Heptasuchus clarki* included.

Heptasuchus clarki was found as a loricatan as the sister-taxon of *Batrachotomus kuperferzellensis*. Tree derived from 72 most parsimonious trees (MPTs) of length (1529 steps) (Consistency Index = 0.335; Retention Index = 0.752)(see supplemental information figure S2).

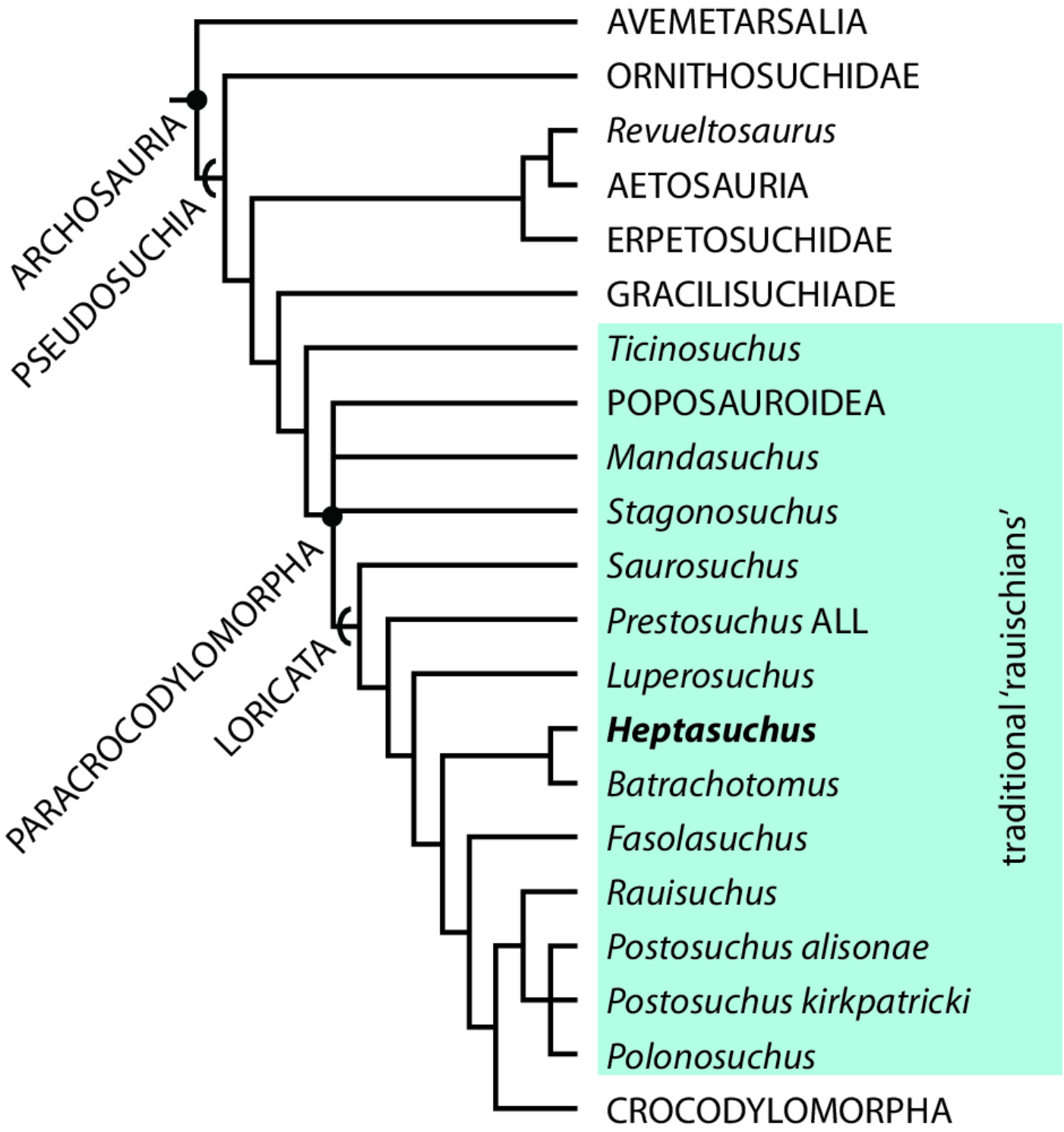
AVEMETARSALIA
ORNITHOSUCHIDAE
Revueltosaurus
AETOSAURIA
ERPETOSUCHIDAE
GRACILISUCHIADE
Ticinosuchus
POPOSAUROIDEA
Mandasuchus
Stagonosuchus
Saurosuchus
Prestosuchus ALL
Luperosuchus
Heptasuchus
Batrachotomus
Fasolasuchus
Rauisuchus
Postosuchus alisonae
Postosuchus kirkpatricki
Polonosuchus
CROCODYLOMORPHA
ARCHOSAURIA
PSEUDOSUCHIA
PARACROCODYLOMORPHA
LORICATA
traditional 'rauischians'

Figure 14

New illustrated character states for paracrocodylomorph archosaurs:

(A) skull referred to *Prestosuchus chiniquensis* (ULBRA-PVT-281) in right lateral view; (B) right postorbital of *Batrachotomus kuperferzellensis* (SMNS 52970) in dorsal (top) and lateral (bottom) view; (C) left postorbital of *Heptasuchus clarki* (UW 11562) in lateral view; (D) left maxilla of *Batrachotomus kuperferzellensis* (SMNS 52970) in medial view; (E) right maxilla of *Heptasuchus clarki* (UW 11562) in medial view; (F) right nasal of *Batrachotomus kuperferzellensis* (SMNS 52970) in lateral view; (G) right nasal of *Heptasuchus clarki* (UW 11562) in lateral view; (H) left maxilla of *Xilousuchus sapingensis* (IVPP V6026) in medial view; (I) right premaxilla of *Heptasuchus clarki* (UW 11562) in lateral view; (J) left premaxilla of *Postosuchus kirkpatricki* (TTUP 9000) in lateral view; (K) left premaxilla of *Xilousuchus sapingensis* (IVPP V6026) in lateral view; (L) right jugal of *Heptasuchus clarki* (UW 11562) in lateral view; (M) right jugal of *Heptasuchus clarki* (UW 11562) in medial view; (N) left jugal of *Batrachotomus kuperferzellensis* (SMNS 52970) in lateral view; (O) left jugal of *Batrachotomus kuperferzellensis* (SMNS 52970) in medial view. Numbers refer to character number separated by a dash from the state. Scales in 10 cm in A, 5 cm in C-G, I, L-M, and 1 cm in B, H, J-K, N-O.

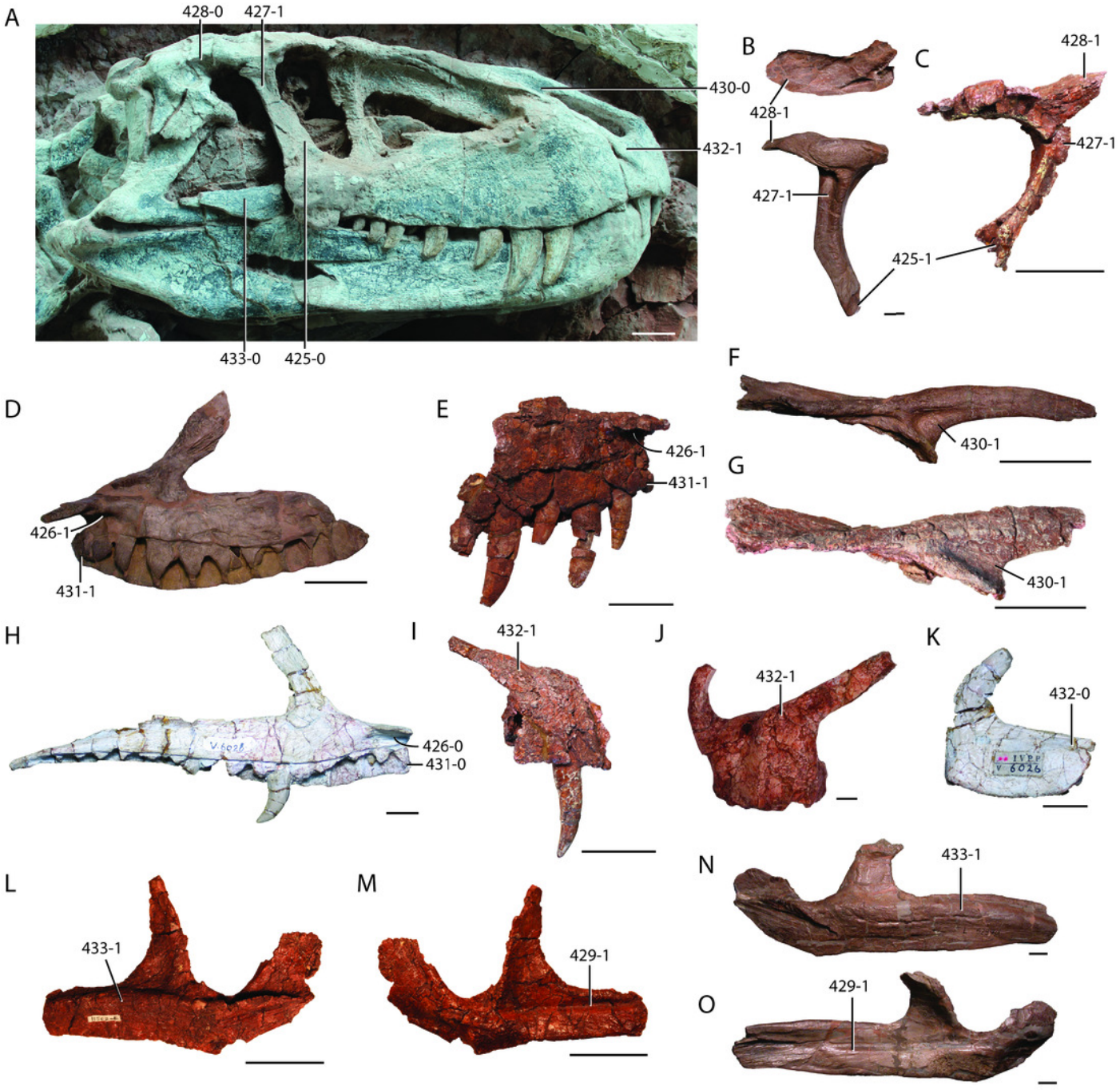
A
428-0
427-1
430-0
432-1
433-0
425-0
B
428-1
427-1
C
428-1
427-1
425-1
D
426-1
431-1
E
426-1
431-1
F
430-1
G
430-1
H
426-0
431-0
I
432-1
J
432-1
K
432-0
L
433-1
M
429-1
N
433-1
O
429-1